

This is an informal report intended for use as a preliminary or working document

# GEND

General Public Utilities • Electric Power Research Institute • U.S. Nuclear Regulatory Commission • U.S. Department of Energy

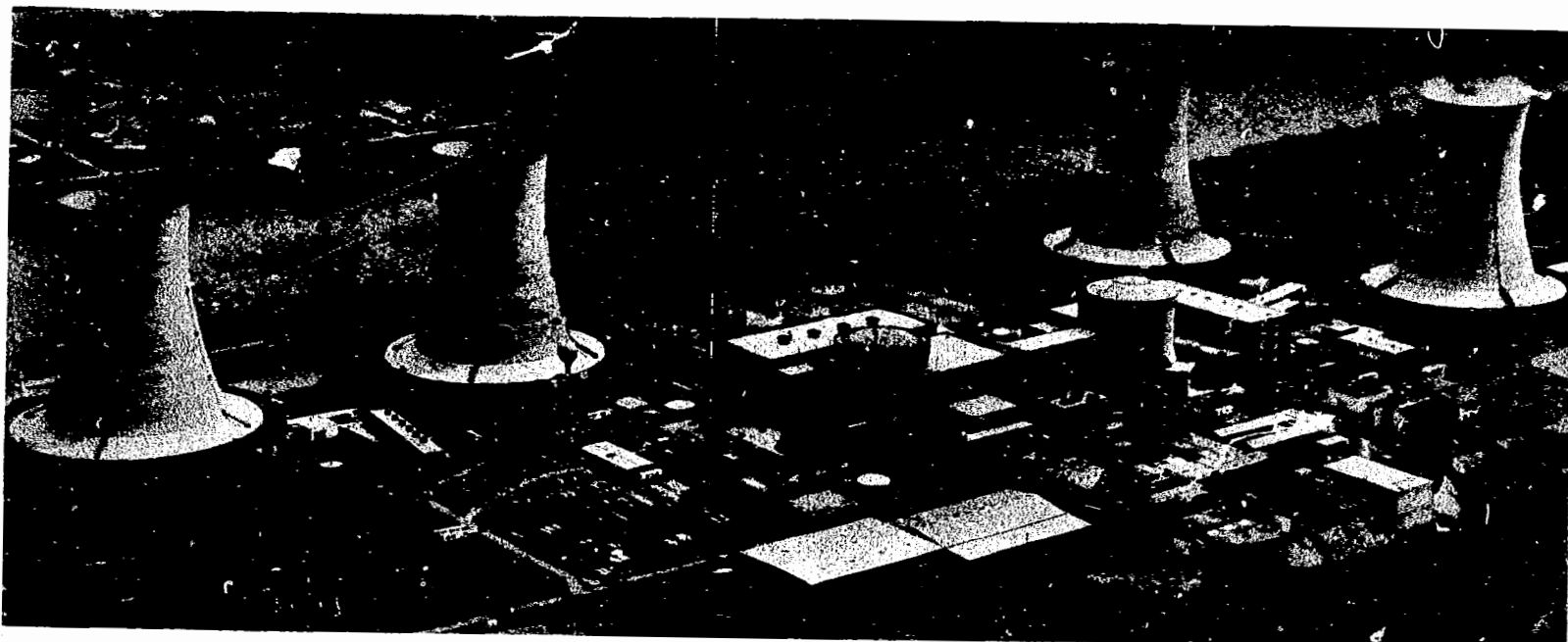
## ASSESSMENT OF EXTENT AND DEGREE OF THERMAL DAMAGE TO POLYMERIC MATERIALS IN THE THREE MILE ISLAND UNIT 2 REACTOR BUILDING

N. J. Alvares

Prepared for the  
U.S. Department of Energy  
Three Mile Island Operations Office  
Under DOE Contract No. DE-AC07-76ID01570

MASTER

DISTRIBUTION OF THIS DOCUMENT IS UNLIMITED



This is an informal report intended for use as a preliminary or working document

# **GEND**

General Public Utilities • Electric Power Research Institute • U.S. Nuclear Regulatory Commission • U.S. Department of Energy

## **ASSESSMENT OF EXTENT AND DEGREE OF THERMAL DAMAGE TO POLYMERIC MATERIALS IN THE THREE MILE ISLAND UNIT 2 REACTOR BUILDING**

N. J. Alvares

Prepared for the  
U.S. Department of Energy  
Three Mile Island Operations Office  
Under DOE Contract No. DE-AC07-76ID01570

**MASTER**

DISTRIBUTION OF THIS DOCUMENT IS UNLIMITED

GEND-INF--023-Vol.6

DE84 010031

**DISCLAIMER**

This report was prepared as an account of work sponsored by an agency of the United States Government. Neither the United States Government nor any agency thereof, nor any of their employees, makes any warranty, express or implied, or assumes any legal liability or responsibility for the accuracy, completeness, or usefulness of any information, apparatus, product, or process disclosed, or represents that its use would not infringe privately owned rights. Reference herein to any specific commercial product, process, or service by trade name, trademark, manufacturer, or otherwise does not necessarily constitute or imply its endorsement, recommendation, or favoring by the United States Government or any agency thereof. The views and opinions of authors expressed herein do not necessarily state or reflect those of the United States Government or any agency thereof.

**ASSESSMENT OF EXTENT AND DEGREE OF  
THERMAL DAMAGE TO POLYMERIC MATERIALS IN  
THE THREE MILE ISLAND UNIT 2 REACTOR BUILDING**

N. J. Alvares

Published February 1984

Lawrence Livermore National Laboratory  
Livermore, California

Prepared for EG&G Idaho, Inc.  
and the U.S. Department of Energy  
Three Mile Island Operations Office  
Under DOE Contract No. DE-AC07-76ID01570

DISTRIBUTION OF THIS DOCUMENT IS UNLIMITED



**Acknowledgments:**

Many people contributed to various sections of this report. From EG&G at TMI; Messrs. Greg Eiden, Doug Reeder, and Jim Jacoby were always helpful and cooperative in supplying information and data about TMI-2 reactor building parameters upon our request. At LLNL; Messrs. Steve Priante and Kirk Staggs did physical measurements of thermal degradation and ease of ignition of exemplar polymers. Messrs. Don Beason and Ken Foote were both actively involved in inspection and analysis of both photographic and extracted items from the reactor building.

## CONTENTS

<b>Abstract</b>	1
<b>Introduction and Background</b>	2
<b>Overpressurization Evidence In and Around the Enclosed Stairwell and Elevator Complex (Northeast) on Both the 305-ft and 347-ft Levels</b>	3
<b>New Work</b>	5
<b>Examination of TMI Materials</b>	8
<b>Thermal Measurements on Exemplar Materials</b>	9
<b>Polar Crane Pendant</b>	12
<b>Hydrogen-Flame-Exposure Tests</b>	13
<b>Conclusions</b>	14
<b>References</b>	16
<b>Appendix A. Calculations</b>	17
<b>Appendix B. Calculations</b>	19
<b>Tables</b>	22
<b>Figures</b>	32

ASSESSMENT OF EXTENT AND DEGREE OF THERMAL DAMAGE  
TO POLYMERIC MATERIALS IN THE THREE MILE ISLAND  
UNIT 2 REACTOR BUILDING

ABSTRACT

Thermal damage to susceptible materials in accessible regions of the TMI-2 reactor building shows damage-distribution patterns that indicate non-uniform intensity of exposure. No clear explanation for non-uniformity is found in existing evidence; e.g., in some regions a lack of thermally susceptible materials frustrates analysis. Elsewhere, burned materials are present next to materials that seem similar but appear unscathed--leading to conjecture that the latter materials preferentially absorb water vapor during periods of high local steam concentration. Most of the polar crane pendant shows heavy burns on one half of its circumferential surface. This evidence suggests that the polar crane pendant side that experienced heaviest burn damage was exposed to intense radiant energy from a transient fire plume in the reactor containment volume. Tests and simple heat-transfer calculations based on pressure and temperature records from the accident show that the atmosphere inside the reactor building was probably 8% hydrogen in air, a value not inconsistent with the extent of burn damage.

Burn-pattern geography indicates uniform thermal exposure in the dome volume to the 406-ft level (about 6 ft below the polar crane girder), partial thermal exposure in the volume between the 406- and 347-ft levels as indicated by the polar crane cable, and lack of damage to most thermally susceptible materials in the west quadrant of the reactor building; some evidence of thermal exposure is seen in the free volume between the 305- and 347-ft levels.

## INTRODUCTION AND BACKGROUND

Ignition of the hydrogen-and-air mixture formed after the breach of the reactor coolant drain-tank rupture disk resulted in nominal thermal and overpressure damage to susceptible materials in all accessible regions of the reactor building. The initiation of burn and the subsequent termination of induced fires are indicated by data from a variety of pressure and temperature sensors located throughout the containment volume. The activation of the building spray system is defined by inflection and increase in the negative slope of interior-temperature-cooling and pressure-reduction curves.<sup>1</sup> Estimates of hydrogen concentration [H] from maximum measured pressure indicate that [H] (in volume %) was <10%. Arguments based on exhaustive analysis of available data suggest that [H] was approximately 8%.<sup>1</sup> At this concentration, propagation of flame is possible upward and horizontally in quiescent conditions, but not downward. However, turbulent conditions, established circulation patterns, and the ambient absolute humidity of the mixture can perturb propagation patterns in ways that are only qualitatively understood.<sup>2,3</sup> Assuming uniform mixing of the 8% mixture and induction of adequate turbulence in internal circulation flows, flame speeds up to 5 m/s are possible--even in the presence of saturated steam environments.<sup>4</sup> Given that no operational ignition sources are available in the reactor building above the 305-ft level, the time delay to achieve peak overpressure is consistent with an ignition location in the basement, especially in view of the basement water spillage and the frequent steam release from the reactor coolant drain-tank pressure-release system.

Internal thermal damage to fine fuels\* indicates the general exposure to fire of all susceptible interior surfaces, with the exception of random items including fabric ties of unknown composition, 2 x 4 framing lumber on both the 305-ft and 347-ft levels, and various polymeric materials. This lack of damage is apparent from photographic and video surveys and has been visually reconfirmed by various entry participants. This pattern is reported in

---

\* Fine fuel is defined as a flammable material with high surface-to-volume ratio.

several informal reports.\* Subsequent entries showed more regions where there is burn damage, but no region where there is unexpected lack of thermal damage. Conjecture as to the reason for these undamaged items includes:

- Preferential absorption of water from saturated atmosphere, increasing the thermal exposure required to produce thermal damage.
- Direct exposure to high-concentration steam and water vapor, resulting in the same effect.
- Shielding from thermal radiation by position or geometric obscuration.
- Shielding from the expanding flame front or convectively driven hot gases by physical obstruction.

OVERPRESSURIZATION EVIDENCE IN AND AROUND  
THE ENCLOSED STAIRWELL AND ELEVATOR COMPLEX  
(NORTHEAST) ON BOTH THE 305-FT AND 347-FT LEVELS

Damage to the elevator and stairwell doors indicates internal pressurization of both the stairwell and the elevator. Moreover, the metal floor plate in front of the elevator door on the 305-ft level was displaced. On the 347-ft level to the east and west side of the enclosed elevator, barrels containing unknown levels of oil were distorted to various degrees.

If the common enclosure for elevator and stairwell communicates directly to the basement, ignition of a near-lower-limit hydrogen-and-air mixture in this volume could produce a damaging pressure differential rate because the containment volume is finite and adiabatic expansion is constrained.<sup>2</sup> Movement of the floor plate on the 305-ft level is possible via pressure reaction from the elevator shaft.

An alternative scenario to explain elevator door distortion is potential H<sub>2</sub> enrichment of the elevator and stairwell enclosure during H<sub>2</sub> production

---

\* Photographs of areas and items discussed in this "Introduction and Background" section are located in Refs. 5 and 6.

periods. Lack of circulation paths could provide a reservoir for a higher-concentration hydrogen-and-air mixture, which would produce a faster local pressure rise--overwhelming the venting capabilities of door gaps.

A third possible pressurization potential results from a temperature rise caused by volumetric flame expansion throughout the reactor building, causing a general pressure increase. For most sites, this pressure rise would correlate directly to flame propagation duration and would equilibrate. However, in relatively tight volumes like the enclosed elevator, the rate of pressure rise may be faster than the venting capabilities of openings, causing the resulting damage.

Damage to the barrels could be overpressure-related and different extents of damage could result from different levels of different contents. However, no other cabinets, tool boxes, dial faces, or electrical boxes indicate unequilibrated pressure distortion in any areas photographed or reported by entry personnel.

Another explanation for observed barrel damage is to attribute distortion to rapid quenching of heated, slightly sealed volumes. Again, the content level and volatility would contribute to degree of distortion. Here, relatively slow heating (duration 10-40 s) can allow gas in the barrel to escape through a poor seal. Upon rapid cooling (from exposure to containment spray systems), interior gases experience pressure reduction. If cooling rate is rapid, inward gas leakage may be frustrated because of pressure enhancement of the seal, and when differential pressure is adequate, permanent distortion results.

Without having the opportunity to closely examine either the subject barrels or the doors to the enclosed elevator and stairwell complex, it is impossible to unequivocally define the processes causing the observed damage. However, on the basis of location and appearance, it is likely that local and independent phenomena (within the total dynamics of hydrogen burn) were responsible for this pressure-related damage evidence.

Most items susceptible to thermal degradation on and above the 347-ft level suffered some photographically apparent thermal damage. On the 305-ft level evidence of burn damage was not extensive. Yet close scrutiny by personnel interested in such observations has found adequate charred and melted items to confirm the presence of a combustion front at most locations on this level.<sup>7</sup> Insufficient photographic or video data is available to

confirm the presence of burn damage below the 305-ft level. However, this region contained most, if not all, of the active electrical circuits that could (either during normal operation or electrical shorting) provide adequate energy for ignition. Since electrical components in reactors are required to be intrinsically safe, it is likely that ignition resulted during arcing failure of an electrical apparatus component, probably in the basement.

#### NEW WORK

Past work in this project focused on identification of burn damage location and patterns at various levels and regions in the containment. The purpose for this assay was to define localized fire-flow patterns and intensity levels, if possible. Although photographic surveys of in-containment vistas, ensembles, items, and surfaces were abundant (approximately 600 photos from 29 entries), clarity of the burn detail in most photographs was not adequate for diagnostic purposes. However, the extent of thermal damage was defined (and is indicated in Figs. 1 through 5) as regions where thermally degraded materials were located, photographed, and, in some cases, extracted from the reactor building for further close examination.

These figures show that thermal damage exists in the following areas:

- The reactor building dome.
- In most free-volume regions above the 347-ft level (except the southeast section).
- In most free-volume regions of the 305-ft level (except the northern and western seismic ring areas).

Areas containing thermally susceptible materials that apparently do not exhibit thermal degradation are:

- The 347-ft level--southeast to southwest along the D-ring.
- The 305-ft level--the region of the equipment hatch and on the northern extent of the fuel storage pond at the containment wall.

To obtain insight into conditions existing before and during the hydrogen burn, temperature records were surveyed from data recorded on a multipoint temperature-measurement system.<sup>8</sup> A summary of these data is presented in Table 1. Data were recorded progressively every 6 min; the times of the transient phenomena were assumed by extrapolation from temperature-change

data. However, good data prior to core uncovering show that lower-level temperatures averaged less than  $100^{\circ}\text{F}$  ( $37.8^{\circ}\text{C}$ ), while dome temperatures were roughly  $130^{\circ}\text{F}$  ( $54.4^{\circ}\text{C}$ ). After core uncovering, temperature in basement areas increased rapidly while dome temperatures remained essentially constant. The cycles of these temperature data are correspondingly similar up to the time of the hydrogen burn. After the hydrogen burn, the dome temperature showed a substantial rise (as did the temperature inside the enclosed stairwell). Throughout this total period, the temperature at the primary reactor shield increased from  $4^{\circ}\text{F}$  to  $10^{\circ}\text{F}$  ( $2^{\circ}\text{C}$  to  $5^{\circ}\text{C}$ ), indicating little thermal or convective energy transfer near the exterior core volume. The average air temperature rise post hydrogen burn\* increased from  $\Delta T = 32^{\circ}\text{F}$  ( $17^{\circ}\text{C}$ ) in regions at or below the 305-ft level to  $\Delta T = 50^{\circ}\text{F}$  ( $25^{\circ}\text{C}$ ) in regions of the dome. This is in direct correlation to both the extent and degree of thermal damage indicated by photographic evidence; i.e., larger free volume, longer flame duration, and fewer heat-loss surfaces contributed to higher average bulk air temperatures in the dome relative to other areas where constrained conditions provided ample heat-loss mechanisms. The same geometric heat-transfer effects should hold true during and after passage of a flame front, and corresponding thermal damage to materials should be complementary.

Ignition of a uniformly distributed near-lower-limit mixture of hydrogen in air, spreading from basement ignition sources to the top of the reactor building dome by turbulent propagation modes, occurred in the time period defined by measured OTSG pressure gauges. The flame front would have been approximately 1 cm thick at an adiabatic flame temperature of about  $1000^{\circ}\text{K}$ .

The exact paths of flame propagation are undefined. Because of the low hydrogen concentration, preferential flame spread was upward in quiescent atmosphere. However, air motion produced by reactor building coolers, steam/hydrogen release from the discharge duct of the reactor-coolant drain tank, and natural convection processes ensured that turbulent flow conditions existed which could greatly modify flame spread rates. The exit of the discharge duct is located near the west open stairway on the undersurface of

---

\* This is temperature rise computed at times just before and after the hydrogen burn.

the 305-ft plane. In Ref. 1, Henri and Postma conclude that the primary paths for entry of the reactor gas mixture to the total reactor building were through the open stairwell. How these gases from the discharge duct interacted with total ventilation patterns is not defined. This may be a moot point since, by the time ignition occurred, hydrogen in the reactor building was undoubtedly uniformly mixed. The ignition source responsible for initiation of the hydrogen burn is undefined. Several circuit boxes, instrument racks, meters, and controllers exist in various locations around D-shields and containment walls in the basement. The heights of these items above the basement floor are undefined. This knowledge is of interest since all electrical service is, by code, designed to be explosion-proof and a potential mode for failure of the circuit components may be by immersion in water. Another ignition source potential is related to the activities of plant operators to control core and reactor building conditions. Activation of valves, pumps, etc. in critical locations could produce ignition arcs from control components perturbed by thermal or mechanical effects of reactor excursion.<sup>9</sup> No obstructions around the inner perimeter of the reactor building block or blind the flow of gases outside of the D-shield. Approximately 10% of the cooled gases from the cooling system plenum (25,000 ft<sup>3</sup>/min) is distributed to this area via committed ducting. The only exit paths for these gases are the seismic gap and the open stairwell. Thus, if ignition occurred from sources away from the open stairwell, the preferred flame propagation path would be upward through the seismic gap. Horizontal spread would occur, but at a slower rate, even during turbulent propagation conditions. As yet, identification of specific ignition sources is not possible from available documentation. However, ample evidence exists on the 347-ft level to confirm flame propagation through the seismic gap regions.

Figure 6 shows photographs of plywood on the reactor building south wall and remains of an instruction or maintenance manual located on the reactor building north wall, both ignited by fire propagation through the seismic gap. Note in Fig. 6a that wires along the wall also exhibit burn trauma. Figures 6c and 6d show the front and rear surface of the plywood panel after it was extracted from the reactor building. Both sides are charred, as are edges and holes through which wire ties penetrate. Surface char condition indicates that the panel ignited to flaming combustion for a short period before self-extinguishing or being quenched by the reactor spray system.

Regardless of the ignition source location, it is apparent that a hydrogen-and-air flame front traversed most of the reactor building volume above (and probably below) the 305-ft level. The duration of this propagation was about 12 s, and thermal exposure to combustible or thermally sensitive surfaces was sufficient to produce thermal damage and/or ignition of these materials, especially in regions where the volume of the combustion plume was optically thick.

The peak pressure rise of about 28 psi during the hydrogen burn indicates that the reaction took place in a mixture of about 8% hydrogen in air. The adiabatic temperature rise during combustion of an 8% hydrogen-in-air mixture is about 1000°K. Calculated exposure radiative and convective flux ( $q_t$ ) from optically thick combustion plumes is:

$$2.2 \text{ W/cm}^2 < q_t < 4.5 \text{ W/cm}^2*$$

This range is approximate since we assume values for combustion plume emittance ( $\Sigma$ ) which may be in error. It is quite possible that  $\Sigma$  could be larger for optically thick hydrogen combustion plumes.<sup>10</sup>

#### EXAMINATION OF TMI MATERIALS

To estimate the intensity of thermal exposure to damaged materials, it is necessary to examine their condition and determine their composition so that thermal damage patterns can be analyzed. Photographic evidence is inadequate for such appraisal. We requested the opportunity to examine materials removed from the reactor building and recommended removal of additional materials for analysis. To date, the following materials have been made available for our examination:

---

\* Appendix A outlines the calculation.

- |  |   |  |
|--|---|--|
| <u>Level 305</u><br><ul style="list-style-type: none"> <li>● Polypropylene bucket</li> </ul> | <u>Level 347</u><br><ul style="list-style-type: none"> <li>● Plywood board</li> <li>● Wood from tool box</li> <li>● Two radiation signs</li> <li>● Hemp and polypropylene rope</li> <li>● Catalog remains</li> <li>● Telephone and associated wire</li> </ul> | <u>Polar Crane</u><br><ul style="list-style-type: none"> <li>● Fire extinguisher</li> <li>● Polar crane pendant and control box</li> </ul> |
|--|---|--|

These materials retain residual radioactive contamination. Consequently, all examination must be performed under rad-safe conditions. Moreover, chemical or physical analytical procedures can only be done on instruments that are contaminated, or can be easily decontaminated. We were unable to locate expendable diagnostic equipment; therefore, our examination of extracted materials was limited to detailed photography and macroscopic observations.

#### THERMAL MEASUREMENTS ON EXEMPLAR MATERIALS

To augment this analysis, we located exemplar materials which are generically similar to those removed from the reactor building. Response properties of the exemplar materials were measured in a thermal gravimetric analyzer (TGA) to ascertain the temperature range of thermal degradation and weight-loss rates. Figures 7, 8, and 9 show TGA patterns for three of these materials:

- NBS-ABS, a standard material used as a control for smoke tests. ABS is acrylonitrile butadiene styrene, similar to telephone body material.
- Electronics terminal material (ABS).
- Red rubber fire hose.

Thermograms are obtained by isothermally heating milligram-sized samples of materials, supported on a micro balance, at a constantly increasing temperature rate. Weight loss with temperature indicates thermal degradation mode and mechanism. Resulting data help identify the material and effects of

additives on thermal behavior. Also, the temperature range of maximum weight loss indicates critical conditions for producing potentially ignitable pyrolyzates.

These figures are included to illustrate how different TGA records can be used to analyze performance of exposure materials. Figure 7 shows that NBS-ABS commences major weight loss at 370<sup>0</sup>C and terminates at 500<sup>0</sup>C. Most flammable pyrolyzates are emitted in this range, leaving about 20% inert material as residue. This material is flammable and, with an external ignition source, it will ignite within this range. Figure 8 shows two major weight-loss periods, the first occurring at 265<sup>0</sup>C and the second at 365<sup>0</sup>C. This ABS formulation included bromine- and antimony-containing fire retardants that release upon pyrolysis to inhibit flaming combustion.

Figure 9 illustrates the thermal degradation pattern for red rubber fire hose. This material begins slow degradation at 211<sup>0</sup>C, ultimately forming an inert char at 470<sup>0</sup>C. We would expect that this material would be difficult to ignite because of low pyrolyzate production.

Table 2 collects TGA data for a variety of materials, some of which are similar to materials extracted from the reactor building. It shows the ranges of temperature required to produce substantial weight loss (and, consequently, pyrolyzate production) from materials. Polymers other than those removed from the reactor building are included because they represent the other kinds of items shown in photographs from the reactor building entry. Also included in Table 2 are the available thermal properties of these materials.

The initial indication of weight loss in TGA generally results from water loss or surface processes. Occurrence of major weight loss from materials results in production of pyrolyzates and both the magnitude and the slope of weight loss indicate the degree of material-destruction processes. The temperature corresponding to the median of weight loss during the first major weight-loss experience can be used to estimate the condition where the rate of thermal destruction is maximum. At this condition it is likely that enough pyrolyzate is produced at the exposure surface to create an ignitable mixture in the boundary layer.

Using standard solutions for transient heat conduction in semi-infinite solids with constant thermal properties, it is possible to calculate the time at which a material's surface will attain a specific temperature upon exposure to constant thermal flux levels. However, adjustments should be made to

account for re-radiation heat losses from exposure surfaces and latent heat processes required to produce pyrolyzates from polymers. With specific surface temperature, exposure heat flux, and defined thermal constants, the time required to reach this temperature is:

$$t = \left( \frac{\pi T_s}{2\dot{q}_t} \right)^2 k \rho c_p . \quad (1)$$

Here  $\dot{q}_t$  is total thermal exposure flux. Times calculated using this equation should be short relative to those for real materials, which experience both thermal and mass convection heat losses. To account for these losses, we adjust  $\dot{q}_t$  by subtracting from it the surface radiation energy at the specified critical surface temperature, and the mass convection losses (the product of surface mass loss rate and latent heat of pyrolysis). The resultant effective energy exposure rate  $\dot{q}_e$  replaces  $\dot{q}_t$  in Eq. (1), giving a longer time to attain the critical temperature level. Values for time obtained by using both  $\dot{q}_t$  and  $\dot{q}_e$  in Eq. (1) bound the time range between exposure of an inert solid and a solid experiencing both re-radiation and latent heat losses. Appendix B outlines this procedure and includes sample calculations for three material types known to be in the TMI-2 reactor building. Critical temperature for the three materials is estimated to be 600°K, and thermal exposure energy is the high value calculated from convective radiative conditions during combustion of 8% hydrogen in air ( $\dot{q}_t = 4.5 \text{ W/cm}^2$ ).

These materials and times to critical weight-loss conditions are:

<u>Material</u>	<u><math>t_e(\dot{q}_t)</math></u>	<u><math>t_c(\dot{q}_e)</math></u>
Pine wood	5.3 s	9.4 s
PVC	32.0 s	54.7 s
Acrylic	40.0 s	68.0 s

Times to attain critical temperature conditions in these materials are of the same order of duration as those recorded during the hydrogen burn in free volumes of the reactor building. Thus, all susceptible materials exposed to this energy should (and did) experience thermal degradation and/or flaming ignition.

## POLAR CRANE PENDANT

One item that possibly received the most intense energy exposure was the pendant and festoon for the polar crane. Figures 10a and 10b show the lower polar crane pendant, and upper polar crane pendant and festoon along the A girder in the reactor building. Figures 10c and 10d, and all plates in Figs. 11, 12, and 13, show the relative thermal damage of cable sections extracted from the reactor building.\* These are illustrative photographs starting from the festoon support of the polar crane and extending to the position of the control box resting on the east side of the west D-shield. A detailed description of thermal damage on each section is contained in Table 3. The figures and tables show that all sections received thermal exposure, including those coiled on the D-shield catwalk. The degree of thermal degradation decreased from the polar crane level to the D-shield top, and, in fact, was only apparent on the bottom pieces where cuts in insulation projected free surfaces of poor heat transfer. Thermal degradation is also apparent on light lenses of the pendant control box (Fig. 13c).

Figure 14 plots thermal damage with pendant length from polar crane level to the top of the D-shield level. Superimposed is the level of  $\beta/\gamma$  radiation (as determined and constructed by Mr. Trujillo). Maximum thermal damage occurs in the region from 6 to 10 ft below the polar crane girder (from about the 420-ft level down to about the 406-ft level). This region shows locally high  $\beta/\gamma$  activity, which may correlate to physical absorption by porous, charred insulation. Thermal damage is severe and circumferentially equal in this region. Char depth on the polymer surface averages 1 to 2 mm. We have no clue as to the composition of the insulating cover for the pendant, so we cannot define the intensity of exposure. However, it was definitely intense and uniform, an indication that this region was bathed for a substantial period in an intense combustion zone.

From the 406-ft level to the top of the D-shield (the 367-ft level), thermal damage is progressively less and becomes more directional; i.e., half

---

\* This examination was conducted at Sandia Laboratories, Albuquerque, in cooperation with Mr. Ralph Trujillo, Project Manager for the cable integrity project for TMI-2 reactor building electrical circuits.

of the insulation circumference exhibited a heavier degree of damage, ranging from char at the 406-ft level to no perceptible insulation degradation just above the D-shield plane. Unfortunately, the direction of exposure is not established, either by cable geometry or by observation. Because of the extent of thermal damage to available polymers in the south and southeast regions of the reactor building, it might be feasible to assume that plume dimensions encompassed that region. Moreover, since all containment gases above the 347-ft level were convected to the air-cooler intake plenums in the southern sector just below the 347-ft level, some preferential fire propagation path may have occurred in this area. However, because there were fewer thermally susceptible materials in the north reactor building regions we cannot contrast the south and north experience to define the center of fire intensity. Had there been either minimal thermal experience or other patterns in susceptible polymers in any other region, we may have had better opportunity to define fire plume geometry. Only one cause for asymmetry of the burn pattern below the 406-ft level can be conjectured: that the cable at this height was exposed to radiation and convection from a hydrogen plume centered to one side (logically the south side) of the reactor building. The exposed surface would sustain flame more readily from the shadowed surface, thus producing the observed pattern.

Photographic documentation of thermal damage patterns sustained by items removed from the TMI-2 reactor building revealed a variety of responses from different materials located in the same general area; e.g., materials around the telephone on the south reactor building wall of the 347-ft level show quite a different response relative to material composition.

#### HYDROGEN-FLAME-EXPOSURE TESTS

Because thermal constants of most polymeric materials are defined only for virgin compounds, it is virtually impossible to calculate thermal response properties. However, simple hydrogen-fire-exposure tests may give an indication of accident exposure conditions. To assess this possibility, we conducted selected exposure tests on our exemplar materials using a Meker burner adjusted to a fully pre-mixed burning mode.<sup>11</sup> Flow was adjusted to produce a measured flame temperature of 833°K (note: during measurement, the

20-mil thermocouple was incandescent, so measured temperature was no doubt substantially lower than actual flame temperature). A simple-copper-slug calorimeter measurement of total thermal flux indicated an exposure flux of  $6 \text{ W/cm}^2$ . This level of flame temperature and thermal flux was close enough to projected TMI-2 accident measurements and estimated reactor exposure conditions, and resulting data trends should be similar to thermal response variations of materials that suffered hydrogen-flame exposure in the TMI-2 reactor building.

Figure 15 shows the simple experimental setup. In Figs. 16 through 24, materials subjected to the experimental fire are compared directly to similar materials extracted from the TMI-2 reactor building. Table 4 gives details of the experimental exposure and descriptions of thermal damage to exposed samples.

Figures 17 through 21 illustrate the correlation between the damage to exemplar and TMI materials of the south-wall telephone stand on the 347-ft level. The similarity of thermal damage is encouraging and the duration and intensity of thermal exposure is in the range of estimated thermal fluxes attained during the reactor building burn. Note that these are very simplistic tests. No attempt was made to refine temperature or thermal energy measurement. Moreover, we had no illusions as to the distribution of convective or radiative contribution from the test burner. However, the results give data trends which are intuitively acceptable. Description of other materials' responses are contained in Table 4.

## CONCLUSIONS

On the basis of

- Photographic and video surveys of the TMI-2 reactor building interior,
- Visual and photographic analysis of materials extracted from the reactor building,
- Macro- and micro-experiments with materials of composition generically similar to that of extracted TMI samples, and
- Calculations using proposed physical conditions and assumed material properties,

the following conclusions are posed:

1. Hydrogen concentration in the reactor building prior to burn was confirmed to be about 8%, as calculated by analyzers of TMI-2 pressure and temperature records.
2. No defined path for hydrogen propagation has been established.
3. Over-pressurization events in the enclosed elevator-and-stairwell complex may be independent of the overall hydrogen-fire-propagation dynamics.
4. The most probable ignition site for the hydrogen burn was in the basement volume; radial location is not defined.
5. Thermal degradation of most susceptible materials on all levels is consistent with direct flame contact from hydrogen fire.
6. Polar-crane-pendant thermal damage indicates intense exposure to a hydrogen-fire plume.
7. The directional character of damage to lower pendant lengths suggests potential geometric limitation of the hydrogen-fire plume.
8. The total burn pattern of the plywood board back for the south-wall telephone on the 347-ft level indicates flame propagation through the seismic gap.
9. Lack of thermal degradation of random, thermally susceptible materials may result from preferential moisture absorption. Because of the random nature of this evidence, it is not likely that undamaged materials resulted from selective shadowing.
10. Burn patterns in the reactor building indicate that the dome region above the 406-ft level was uniformly exposed to direct hydrogen flame, the region between the 406-ft level and the top of the D-shield was partially exposed to hydrogen flame (most likely in the south and east quadrants), and the damage on the 305-ft level was geometrically similar to that above the 347-ft level but of less degree.

## REFERENCES

1. J. O. Henrie and A. K. Postma, Analysis of the Three Mile Island (TMI-2) Hydrogen Burn, Rockwell International, Rockwell Hanford Operations, Energy Systems Group, Richland, WA, RHO-RE-SA-8 (1982).
2. M. Hertzberg, Flammability Limits and Pressure Development in H<sub>2</sub>-Air Mixtures, Pittsburg Research Center, Pittsburg, PA, PRC Report No. 4305 (1981).
3. Flame and Detonation Initiation and Propagation in Various Hydrogen-Air Mixtures, With and Without Water Spray, Rockwell International, Atomics International Division, Energy Systems Group, Canoga Park, CA, A1-73-29.
4. W. E. Lowry, B. R. Bowman, and B. W. Davis, Final Results of the Hydrogen Igniter Experimental Program, Lawrence Livermore National Laboratory, Livermore, CA, UCRL-53036; U. S. Nuclear Regulatory Commission, NUREG/CR-2486.
5. G. R. Eidem and J. T. Horan, Color Photographs of the Three Mile Island Unit 2 Reactor Containment Building: Volume 1--Entries 1, 2, 4, 5, 6, U. S. Nuclear Regulatory Commission, Washington, DC, GEND 006 (1981).
6. N. J. Alvares, D. G. Beason, and G. R. Eidem, Investigation of Hydrogen Burn Damage in the Three Mile Island Unit 2 Reactor Building, U. S. Nuclear Regulatory Commission, Washington, DC, GEND-INF-023 Vol. I (1982).
7. R. Trujillo, private communication, November 1982.
8. J. K. Jacoby, R. A. Nelson, C. L. Nalezny, and R. H. Averill, Data Integrity Review of Three Mile Island Unit 2 Hydrogen Burn Data, EG&G, Inc., Idaho Falls, ID (1982).
9. T. L. VanWitbeck and J. Putnam, Annotated Sequence of Events, March 28, 1979, GPU Nuclear, TDR-044 (1981).
10. M. Hertzberg, A. L. Johnson, J. M. Kuchta, and A. L. Furno, "The Spectral Radiance Growth, Flame Temperatures, and Flammability Behavior of Large-Scale, Spherical, Combustion Waves," Proceedings of the Sixteenth Symposium (International) on Combustion, The Combustion Institute, Pittsburgh, PA (1976).
11. B. Lewis and G. von Elbe, Combustion, Flames and Explosions of Gases, 2nd ed. (Academic Press, Inc., New York, NY, 1961), p. 490.

Appendix A  
CALCULATION FOR RADIANT EXPOSURF ENERGY

Assume:  $T_{max} \approx 1400^{\circ}\text{F}$  ( $\approx 1000^{\circ}\text{K}$ )

$$q_r = \sigma GT \quad 0.2 < \sigma < 0.8$$

$$\sigma = 5.665 \times 10^{-5} \text{ erg/cm}^2\text{sec}^{-1}\text{K}^4$$

$$T^4 = 10^{12}\text{K}^4$$

$$\sigma T^4 \approx 5.7 \times 10^7 \text{ erg/sec cm}^2$$

$$1 \text{ joule} = 10^7 \text{ erg}$$

$$1 \text{ joule/sec} = \text{watt}$$

$$q_{r(\sigma=1)} = 5.7 \text{ watt/cm}^2$$

$$q_{r(\sigma=0.8)} = 4.6 \text{ watt/cm}^2$$

$$q_{r(\sigma=0.2)} = 1.1 \text{ watt/cm}^2$$

Since only emission during  $\text{H}_2$  combustion in OH and  $\text{H}_2\text{O}$  bands for optically thick water vapor at  $1000^{\circ}\text{K}$   $\sigma < 0.5^*$   
 $\sigma < 0.6^{\dagger\dagger}$

$$q_{r(\sigma=0.5)} = 2.85 \text{ watt/cm}^2$$

---

\* Eckert, Introduction to Heat and Mass Transfer, p. 243.  
 † Giedt, Principles of Engineering Heat Transfer, p. 265.

## CALCULATION FOR CONVECTIVE HEAT TRANSFER COEFFICIENT ( $\bar{h}$ ) RANGE

Use properties of Hot Air:  $T \approx 1000^{\circ}\text{K}$ ,  $T_{\text{amb}} = 311^{\circ}\text{K}$

Velocity Range:  $10 \text{ ft/sec} < U_{\infty} < 40 \text{ ft/sec}$   
 Assume  $1 = 1.0 \text{ ft}^2$

$$\bar{h} = 0.664 \cdot K \cdot \frac{Pr^{1/3}}{v^{1/2}} \quad K = 3.9 \times 10^{-2} \frac{\text{BTU}}{\text{hr ft } ^{\circ}\text{F}}$$

$$Pr = 0.702$$

$$(Pr)^{1/3} = 0.89$$

$$v = 126.8 \times 10^{-5} \frac{\text{ft}^2}{\text{sec}}$$

$$\frac{U_{\infty}}{\bar{h}} = 10 \text{ ft/sec}$$

$$\bar{h} = 1.16 \times 10^{-3} \text{ watt/cm}^2 {}^{\circ}\text{K}$$

$$\dot{q} = \bar{h}A (T_s - T_{\infty})$$

$$\dot{q}_c = 0.8 \text{ watt/cm}^2$$

$$\frac{U_{\infty}}{\bar{h}} = 40 \text{ ft/sec}$$

$$\bar{h} = 2.33 \times 10^{-3} \text{ watt/cm}^2 {}^{\circ}\text{K}$$

$$\dot{q} = \bar{h}A (T_s - T_{\infty})$$

$$\dot{q}_c = 1.6 \text{ watt/cm}^2$$

## RANGE OF THERMAL FLUX BASED ON 8% HYDROGEN

$$\dot{q}_T = \dot{q}_r + \dot{q}_c(\text{min}) 1.4 + 0.8 \approx 2.2 \text{ watt/cm}^2$$

$$\dot{q}_T = \dot{q}_r + \dot{q}_c(\text{max}) 2.85 + 1.6 \approx 4.45 \text{ watt/cm}^2$$

(Experimentally determined thermal flux from small premixed source.  
 $\dot{q}$  measured; Meeker burner = 6 watt/cm<sup>2</sup>)

Appendix B  
TIME ESTIMATE FOR CRITICAL TEMPERATURE RISE

Temperature distribution in panel exposed to external heat flux described by:

$$(1) \frac{\partial T}{\partial t} = \alpha \times \frac{\partial^2 T}{\partial y^2}$$

Assume heat loss from surface dependent on surface temperature, then, surface boundary condition is:

$$-K_s \frac{\partial T}{\partial y} \quad \sim \text{Exposure Flux} \\ (0, t)$$

Assuming constant solid thermal parameters and temperature rise at irradative surface ( $y = 0$ );

Simplified solution to equation 1 is:

$$\Delta T(0, t) = \left( \frac{2q_T}{\pi K_p C_p} \frac{t}{y} \right)^{1/2}$$

solve for  $t$ :

$$t = \left( \frac{\pi}{2} \frac{T_s}{q_T} \right)^2 K_p C_p$$

This form gives estimate of time for specific temperature rise in inert solid before temperature rise reaches back surface.

ACCOUNT FOR HEAT LOSS DUE TO RE-RADIATION  
FROM SURFACE AND LATENT HEAT PROCESS

Approximate surface temperature for production of ignitable pyrolyzates is 600<sup>0</sup>K. Thus, for most pessimistic case for reradiation losses:

$$\dot{q}_{rr} = \Sigma T^4 = 0.74 \frac{\text{watt}}{\text{cm}^2}$$

Latent heat to convert solid to gas and critical mass flux at mean temperature of maximum weight loss for materials in table 2 (about 600<sup>0</sup>K) are of order 2kW/gm and 2 x 10<sup>-4</sup>gm/cm<sup>2</sup> sec respectively;\* therefore, heat lost due to latent heat processes is:

$$\dot{q}_{(lat)} = 2 \times 10^5 \frac{\text{W} \cdot \text{sec}}{\text{gm}} \times 2 \times 10^{-4} \frac{\text{gm}}{\text{cm}^2 \text{sec}}$$

$$\dot{q}_{(lat)} = 0.4 \frac{\text{watt}}{\text{cm}^2}$$

Thus, maximum heat loss from surface at critical mass loss flux temperature is:

$$q_{rr} + q_{lat} = 0.74 + 0.4 = 1.14 \frac{\text{watt}}{\text{cm}^2}$$

---

\* A. Tewarson, Physico-chemical and Combustion Pyrolysis Products of Polymeric Materials, National Bureau of Standards, Washington, DC,  
NBS-GCR-80-295 (1980).

TIME TO RAISE SURFACE TEMPERATURE TO CRITICAL MASS PRODUCTION LEVEL

PVC--Generic

$$t_i = \left( \frac{\pi}{2} \frac{T_s}{q_T} \right)^2 K \rho C_p$$

$\rho = 1.2 \text{ gm/cm}^3$   
 $C_p = 1.4 \frac{\text{joule}}{\text{gm} \cdot {}^\circ\text{K}}$   
 $K = \frac{14.6 \times 10^{-4} \text{ joule}}{\text{cm}^2 \text{ sec } {}^\circ\text{K}}$   
 $t_i = 32.0 \text{ sec}$   
 (inert solid)

$\Delta T_S = 623^\circ\text{K} - 300 = 323^\circ\text{K}$   
 $t_i = 54.7 \text{ sec}$   
 (include losses)

$q_T = 4.45 \text{ joule/cm}^2 \cdot \text{sec}$

Pine Wood

$\rho = 0.34 \text{ gm/cm}^3$   
 $C_p = 1.4 \frac{\text{joule}}{\text{gm} \cdot {}^\circ\text{K}}$   
 $K = \frac{8.8 \times 10^{-4} \text{ joule}}{\text{cm}^2 \text{ sec } {}^\circ\text{K}}$   
 $t_i = 5.3 \text{ sec}$   
 (inert solid)

$\Delta T_S = 323^\circ\text{K}$   
 $t_i = 9.4 \text{ sec}$   
 (include losses)

$q_T = 4.45 \text{ joule/cm}^2 \cdot \text{sec}$

PMMA (Acrylic)

$\rho = 1.17 \text{ gm/cm}^3$   
 $C_p = 1.3 \frac{\text{joule}}{\text{gm} \cdot {}^\circ\text{K}}$   
 $K = \frac{20 \times 10^{-4} \text{ joule}}{\text{cm}^2 \text{ sec } {}^\circ\text{K}}$   
 $t_i = 40.0 \text{ sec}$   
 (inert solid)

$\Delta T_S = 323^\circ\text{K}$   
 $t_i = 68.0 \text{ sec}$   
 (include losses)

$q_T = 4.45 \text{ joule/cm}^2 \cdot \text{sec}$

Table 1. Record of temperatures at various points in the reactor building.

Thermocouple and location	Ambient temp prior to 0400 March 28	Time of incident (steam release)	Initial temperature rise (°F)	Differential temperature resulting from steam release (°F)	Time mark		Pre-burn background temperature (°F)	Pre-burn air temperature change relative to pre-steam release (°F)	Post-burn air temperature (°F)	Post-burn bulk temp rise (°F)
					just before ignition	Next time mark				
A-12 AH-TE-5022: Top ceiling ambient air (R-7), 353 ft	120	0447	120	0	1347	1353	128	08	180	52
A-13 AH-TE-5022: Top ceiling ambient air, southeast	120	0454	119?	0	1348	1354	125	05	182	57
A-14 AH-TE-5023: West end stair- well (R-5)	119	0447	130	21	1347	1353	128	09	170	42
A-15 AH-TE-5027: Air conditioner plenum outlet	86	0446	85	0	1346	1352	80	06	122	42
A-16 AH-TE-5088: Southeast stairwell (R-18A), 310 ft	100	0442	100	0	1348	1354	106	06	151	45
A-1 AH-TE-5010: Sump pump, 282 ft	91	0452	113	22	1346	1352	107	16	132	25
A-2 AH-TE-5011: Let-down cooler ambient air, 282 ft	88	0452	115	27	1346	1352	102	14	128	26
A-3 AH-TE-5012: Reactor coolant drain tank, 282 ft	87	0447	152	65	1347	1353	118	31	152	34
A-4 AH-TE-5013: Impinge bar ambient air, 232 ft	92	0452	108	16	1346	1352	116	24	156	40

Table 1. (Continued.)

Thermocouple and location	Ambient temp prior to 0400 March 28	Differential temperature				Pre-burn air temperature				Post-burn bulk temp rise (°F)
		Time of incident (steam release)	Initial temperature rise (°F)	resulting from steam release (°F)	Time mark just before ignition	Next time mark	Pre-burn background temperature (°F)	change relative to pre-steam release (°F)	Post-burn air temperature (°F)	
A-5 AH-TE-5014: N.R. equipment hatch, 305 ft	103	0442	105	02	1348	1354	117	14	151	34
A-6 AH-TE-5015: Air conditioner plenum outlet, 319 ft	78	0445	111	33	1345	1351	78	0	124	46
A-7, A-8, A-9, A-10, AH-TE-5016-5019: Primary shield ambient air, 282 ft	102-110	(Temperature rise over entire event increases from 4°F to 10°F)								
A-11 AH-TE-5020: Top ceiling ambient air (R-15)	127	0447	128	01	345					
									Average: 40.3	

Table 2. Data from thermogravimetric analysis of materials removed from the reactor building and of exemplar materials.

24

Sample	Temperature at initial weight loss (°C)	First major weight-loss stage (°C)	% Sample wt loss	Median temp during first wt-loss stage (°C)	Weight % ash at °C	Thermal conductivity (10 <sup>-4</sup> cal·cm/s·cm <sup>2</sup> ·°C)	Specific gravity	Specific heat (cal/g·°C)
Safety glasses frame (probably polyethylene)	100	252-450	87.2	351	0 at 550			
Telephone <sup>a</sup> body (see ABS-NBS)	60	378-523	89.5	450	0 at 650			
ABS electronic instrument panel	150	265-365	30.1	315	4.0 at 600		1.03-1.06	0.36
NBS-ABS	60	370-500	77.7	435	9.0 at 700		1.03-1.06	0.36
Telephone wire <sup>a</sup> (possible PVC)	30	232-352	63.7	292	0 at 750			
Rubber hose <sup>a</sup>	30	211-470	37.5	340	41 at 850			
Acrylic from telephone dial <sup>a</sup>	70	409-549	72.1	479	0 at 650	4-6	1.17-1.20	0.35
Wood (fir) <sup>a</sup>	30	281-373	58.8	327	0 at 550		0.3-0.6	0.34
Tygon tubing <sup>a</sup>	150	228-406	78.5	317	0 at 650	3-4	1.16-1.35	
Acrylic sheet	250	451-522	71.0	486	0 at 650	4-6	1.17-1.20	0.35
Nylon wire insulation	40	380-467	88.2	423	0 at 600	5	1.06-1.08	0.40
Foam polystyrene	100	392-495	95.2	443	1.1 at 600			
PVC wire #1	110	245-410	29.0	327	4.5 at 650	3-4	1.3-1.7	
PVC wire #2	150	252-400	60.3	326	9.2 at 650	3-4	1.3-1.7	
PVC telephone <sup>a</sup> receiver cord	160	253-405	56.6	329	15.8 at 850	3-4	1.3-1.7	

Table 2. (Continued.)

Sample	Temperature at initial weight loss (°C)	First major weight-loss stage (°C)	% Sample wt loss	Median temp during first wt-loss stage (°C)	Weight % ash at °C	Thermal conductivity ( $10^{-4}$ cal·cm/s·cm $^2$ ·°C)	Specific gravity	Specific heat (cal/g·°C)
Polypropylene TV antenna cable	240	299-434	83.5	366	0.5 at 550	3.5-4	0.89-0.91	
Polyethylene wire jacket	220	323-468	90.6	395	0 at 550		0.91-1.4	0.55
Caution sign <sup>a</sup> (probably polyethylene)	50	252-453	88.7	352	0 at 550			

<sup>a</sup> Exemplar material.

Table 3. Thermal damage to sections of the polar crane pendant.

Section No.	Length (in.)	Damage
31	20	North side ash, plastic tape char all around, no degradation under tape
30	28	Half circumference char, half ash (ash grey, char black)
29	31	Low end complete char for 15 in., 180° char/ash to top <sup>a</sup>
28	25-1/4	Char complete circumference
27	32-3/4	Circumferential char for total length, depth ~1-2 mm
26	29-1/2	Circumferential char for total length
25	31	Circumferential char for total length
24	30	Circumferential char, marked side ash for top 15 in., 2/3 ash and 1/3 char on bottom end
23	30	Char 120° for top 20 in., ash 25° (marked side)
22	30	180° ash on marked side--slight thermal damage on remaining circumference
21	29-1/2	120° ash on marked side--slight damage
20	31	Same as No. 21
19	29-1/2	180°char and 180° ash for top 21.5 in., extraneous char on low end, extraneous deposited material ~6" long starting at 6 in. from low end and twisting up to char
18	31	Ash opposite marked side, but little thermal damage on unmarked side
17	30	Same as No. 18
16	29	Same as No. 18
15	29-1/2	120° light ash on total length of section, opposite marked side
14	30-1/2	Same as No. 15
13	30-1/2	Same as No. 15 but grade to lighter damage

Table 3. (continued)

Section No.	Length (in.)	Damage
12	29	No clear ash or thermal damage
11	31-1/2	No char, no ash except for char on deposited material, drips, etc.
10	30	Same as No. 11
09	29-1/2	No char, no ash; first pliable piece
08	30	No char or ash on surface, two cuts exhibit char on inside surface and inner conductors, flexible 9-10.5 in. from low end
07	31-1/2	One cut 3-1/2 in. from low end, tip charred, no apparent inner degradation
06	30	Flexible, no char, no ash
03 to 05	94	Splice and insulation checks and cuts
01 to 02	56	Circumferential burn pattern from tape or paper wrapped around piece 8-10 in. from No. 2 end

<sup>a</sup> Degrees refer to portion of circumference of cable.

Table 4. Results of hydrogen-fire-exposure tests on exemplar materials.

Sample	Test	Time (s)	Energy exposure (J/cm <sup>2</sup> )	Results of exposure
Polypropylene rope	1	12	72	Melted at ends, waxy
	1A	30	180	More melting at ends than test 1, some blending of materials
	1B	27	162	Melting at point of contact, breakage occurred at 27 s into test with moderate pulling force applied
	1C	33	198	More melting than test 1B, breakage occurred at 33 s into test with very little force applied
Telephone receiver cord	2	12	72	Melting, fusing of jacket, conductors exposed, bubbling of clear plastic plug
	2A	30	180	More melting of jacket than test 2, char formation, signs of dripping, conductors exposed and ignited at 29 s into test
Telephone dial	3	12	72	Melting at edges, some bubbling
	3A	20	120	Melting at edges, incipient bubbling
Telephone dial (on screen)	4	30	180	(Material placed on screen to prevent dripping onto burner): Melted into screen, bubbling
	4A	20	unknown	(Inadvertent flame temp. decrease approx. 30-40°C): Bubbling.
	4B	35	unknown	(Inadvertent flame temp. decrease approx. 30-40°C): More bubbling than 4A

Table 4. (continued)

Sample	Test	Time (s)	Energy exposure (J/cm <sup>2</sup> )	Results of exposure
Telephone extension line	5	12	72	Melting, charring along edge of cable, bubbling and deformation of clear plastic plug
	"	5A	20	More charring and melting than in test 5--ignited approximately 18 s into test
Plywood	6	12	71	Some charring along edges of plywood
"	6A	20	120	More charring than in test 6, minimal burning through top lamina
"	6B	30	180	More charring of top surfaces, outer edges and corners; splitting of top layer
"	6C	60	360	Extreme charring of top surface and sides, ashy appearance at corners
Plywood (wet)	7	12	72	No noticeable change
"	7A	30	180	Slight char along one edge
"	7B	60	360	Charring approximately like test 6B
ABS (white material)	8	12	72	Loss of strength, bubbling, slight char, deformation
	"	8A	20	More bubbling, deformation, blackening of approx. 74% of surface area
ABS (on screen)	8B	30	180	More bubbling, melted edges, melted into screen, brownish color over surface
"	8C	40	240	Bubbling, melted edges, melted into screen, brownish color over surface

Table 4. (continued)

Sample	Test	Time (s)	Energy exposure (J/cm <sup>2</sup> )	Results of exposure
Duct tape	9	12	72	Widespread bubbling, penetration through top (silver) layer
"	9A	20	120	More bubbling than in test 9, penetration through top layer
"	9B	30	180	More bubbling, charring, melting of adhesive, penetration through top layer
Plywood covered with PE	12	12	72	(Plywood covered with single layer of polyethylene one side only): PE burned completely away, charring on two opposite edges
"	12A	12	72	(Plywood covered with a double layer of PE on one side only): 25% of PE lost due to drippage and shrinkage, charring along edges of plywood
"	12B	20	120	(Double layer of PE on one side of plywood): PE burned completely away, charring at edges and corners of plywood; PE ignited at 15 s into test, and one edge of the plywood ignited also
"	12C	12.5	75	(Wood placed in PE bag): Bag burned away at approximately 7 s; noticeable color change in wood at approximately 12.5 s
"	12D	9.5	57	(Plywood placed in PE bag): Bag burned away approximately 6 s into test; noticeable color change in plywood at approximately 9.5 s
"	12E	13	78	(Plywood placed in PE bag): Bag burned away approximately 6 s into test; noticeable color change in plywood at approximately 13 s (this plywood was a darker piece than used in test 12D)

Table 4. (continued)

Sample	Test	Time (s)	Energy exposure (J/cm <sup>2</sup> )	Results of exposure
Telephone body	10	12	71	Loss of strength, some wrinkling
"	10A	20	120	Leathered appearance, bubbling
"	10B	30	180	More bubbling; otherwise same as 10A
Hose	11	12	72	No noticeable change
"	11A	20	120	No noticeable change
"	11B	30	180	Some discoloration
"	11C	60	360	Charring, slight deformation, melting of outer covering

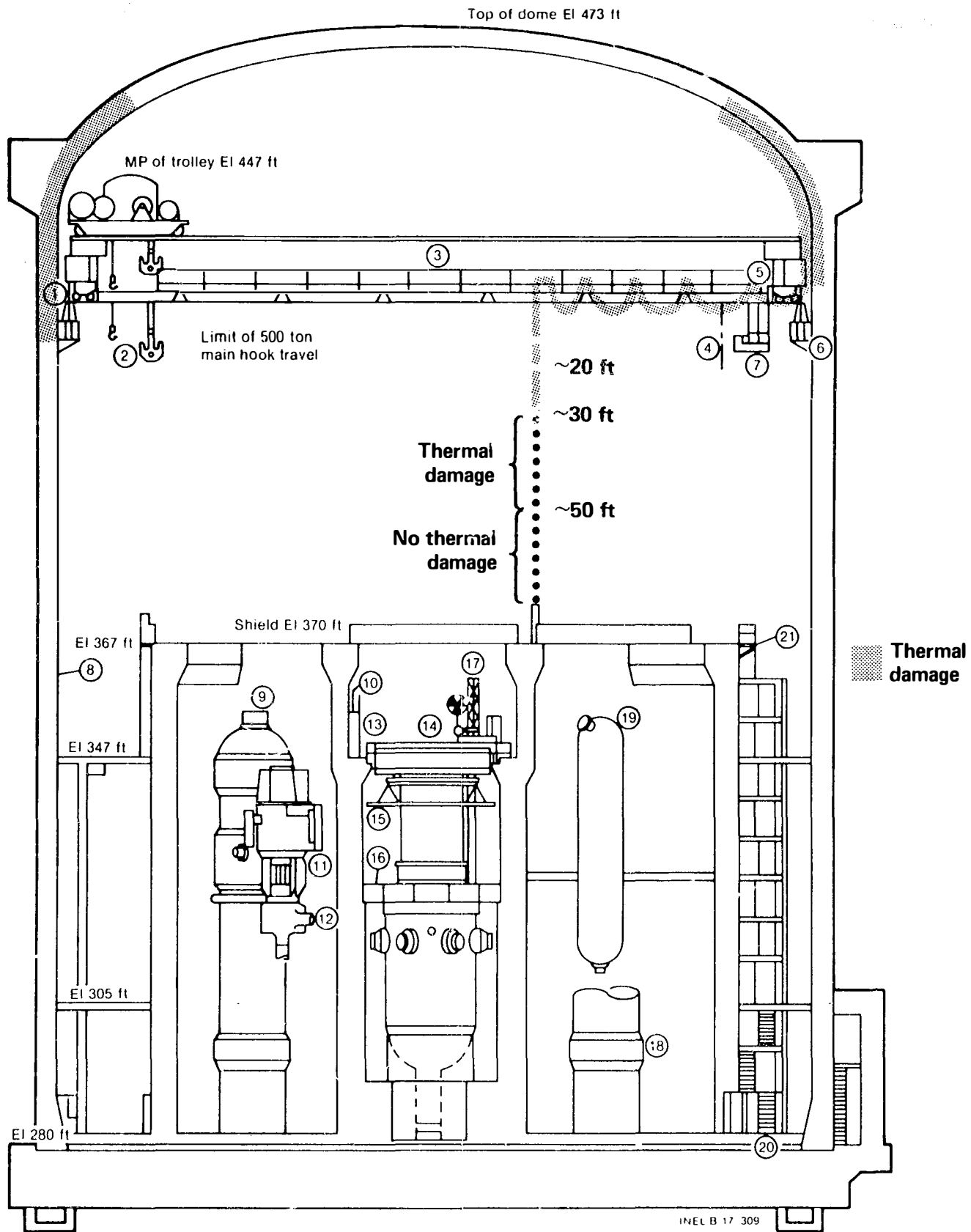


Figure 1. Cross section of the TMI-2 reactor containment building.

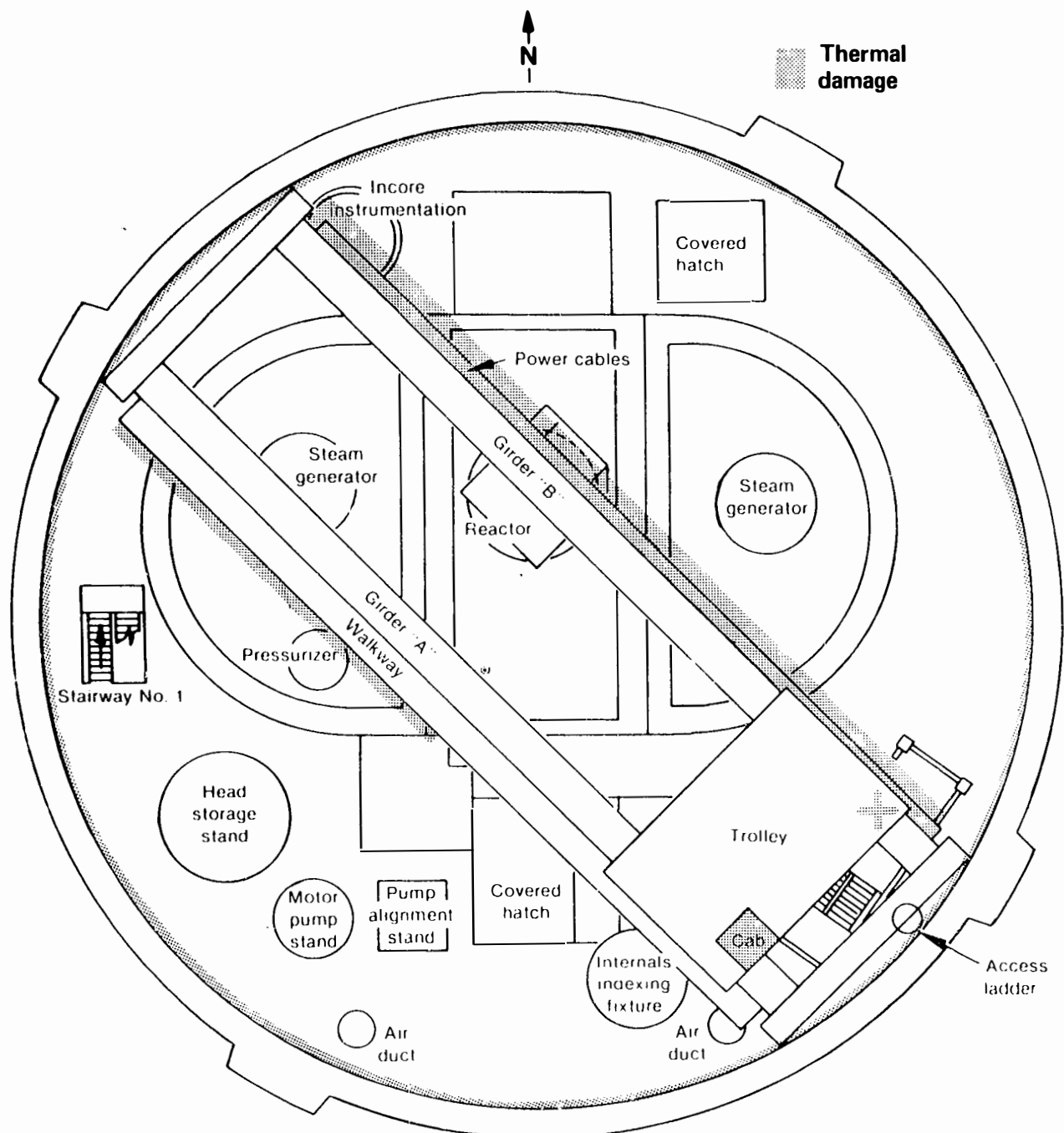


Figure 2. Thermal damage on the 347-ft level (with polar crane superimposed).

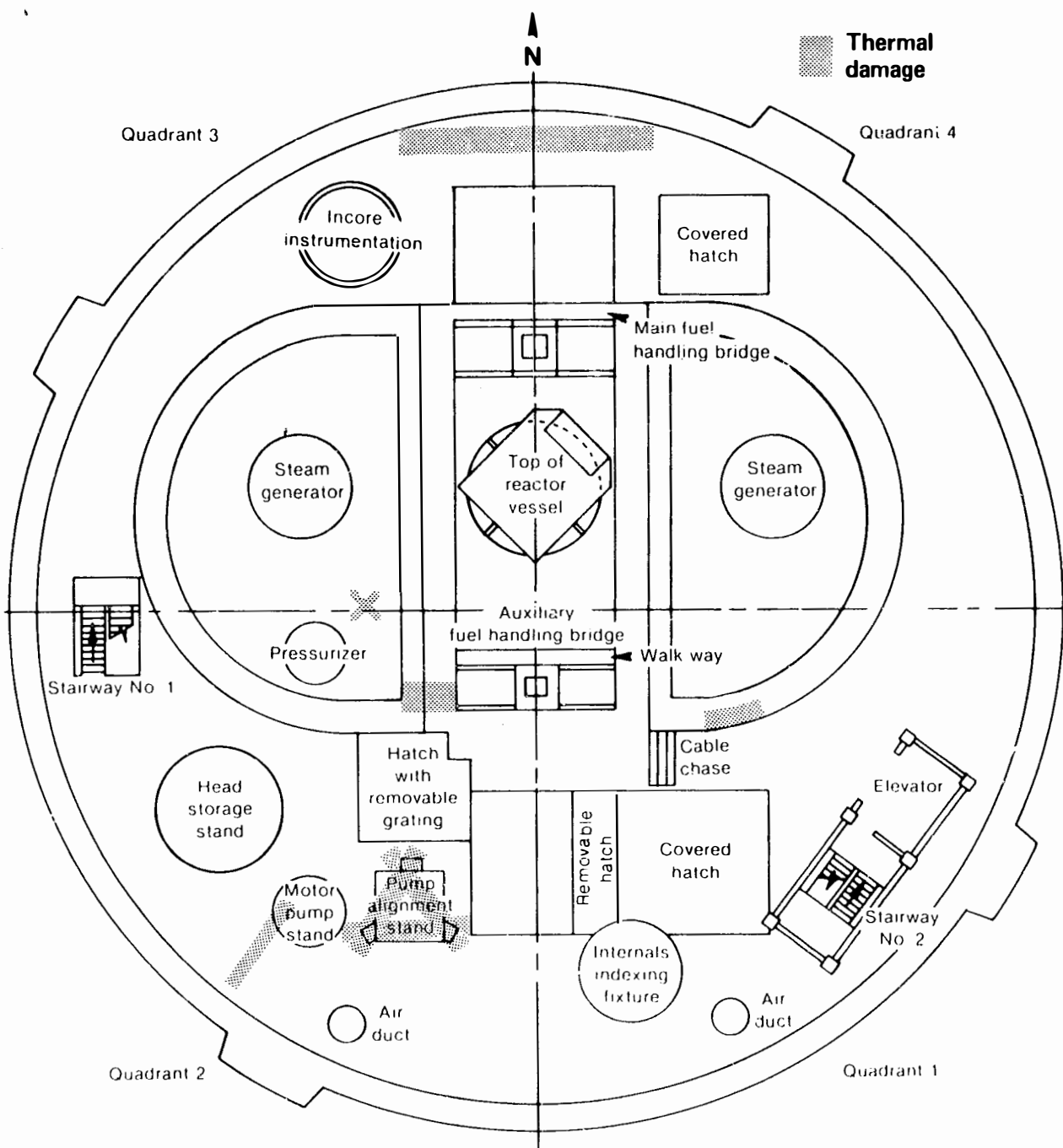


Figure 3. Thermal damage in the same plane as the D-rings.

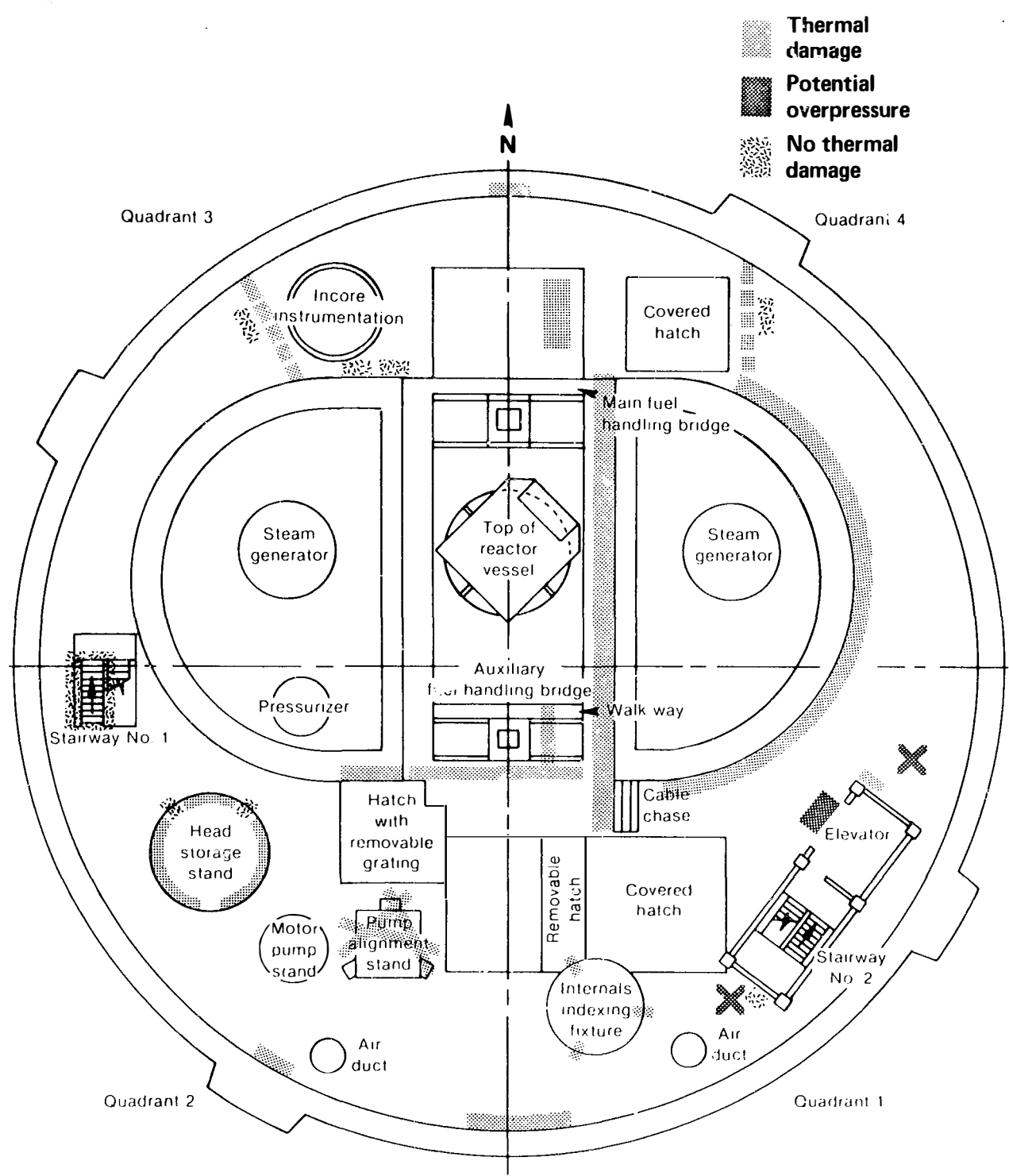


Figure 4. Thermal damage and potential overpressure on the 347-ft level.

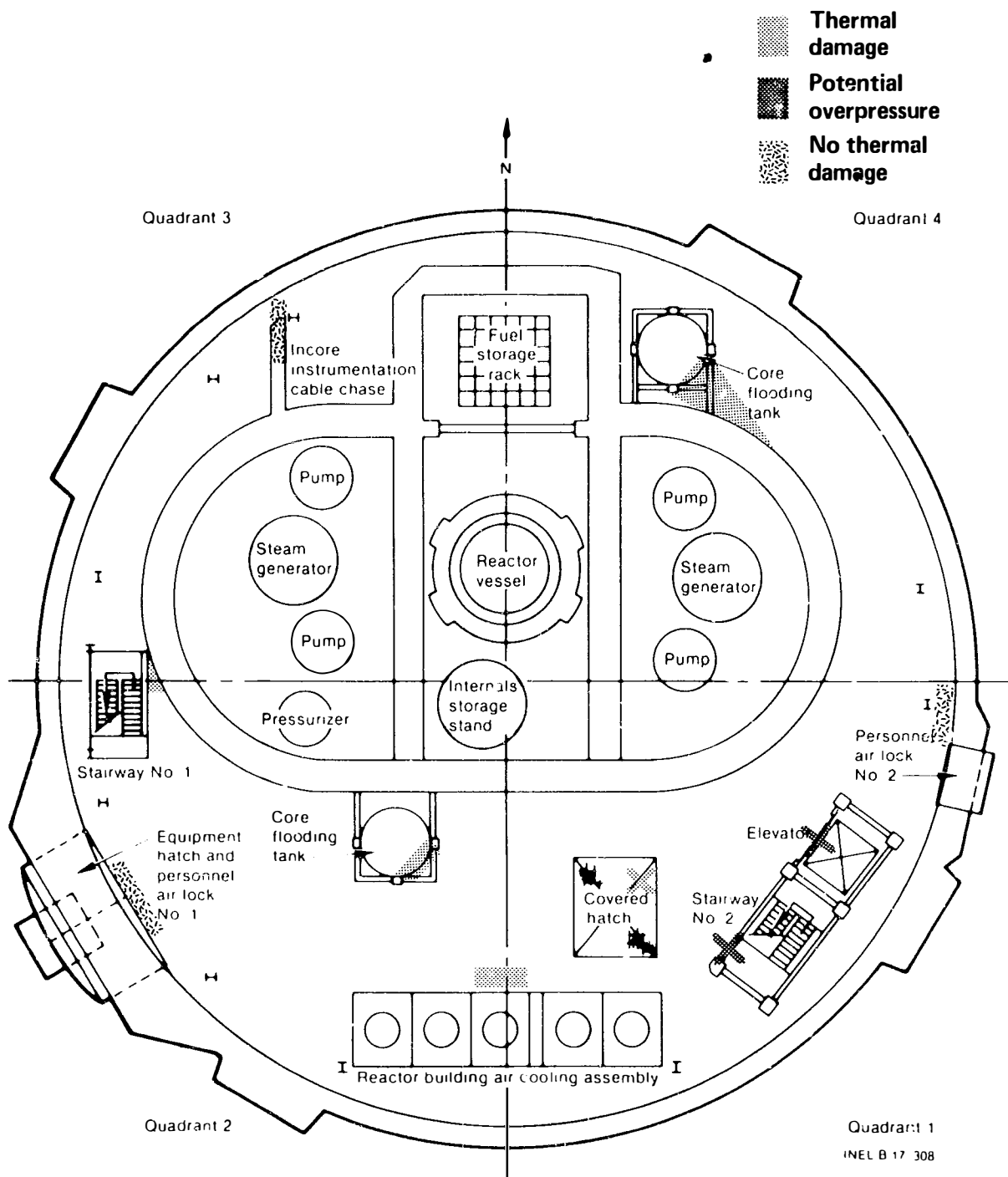
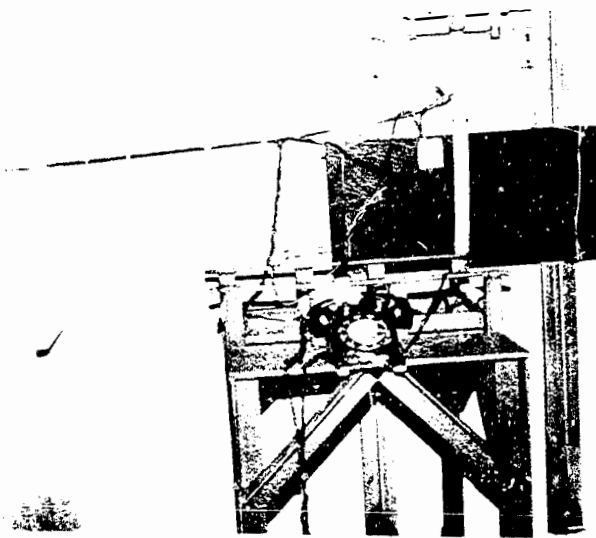


Figure 5. Thermal damage and potential overpressure on the 305-ft level.

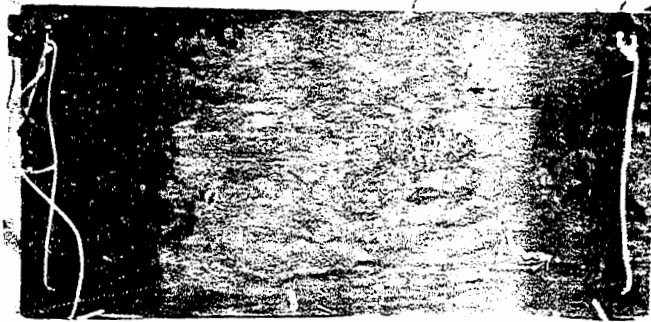
(a)



(b)



(c)



(d)

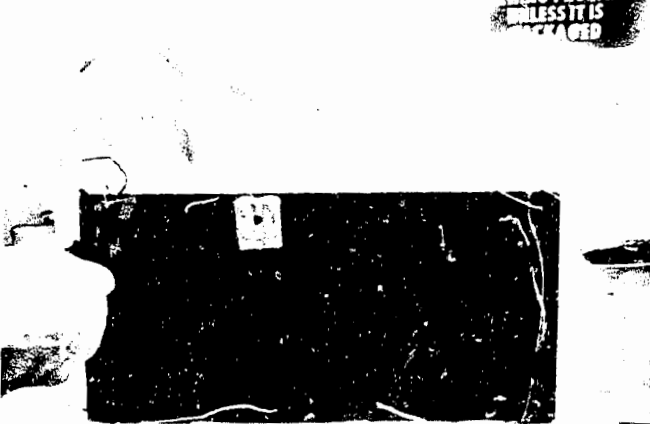


Figure 6. Hydrogen-burned in-containment materials: (a) Bell telephone. (b) Charred manual on electrical box. (c) Back of plywood panel. (d) Front of plywood panel.

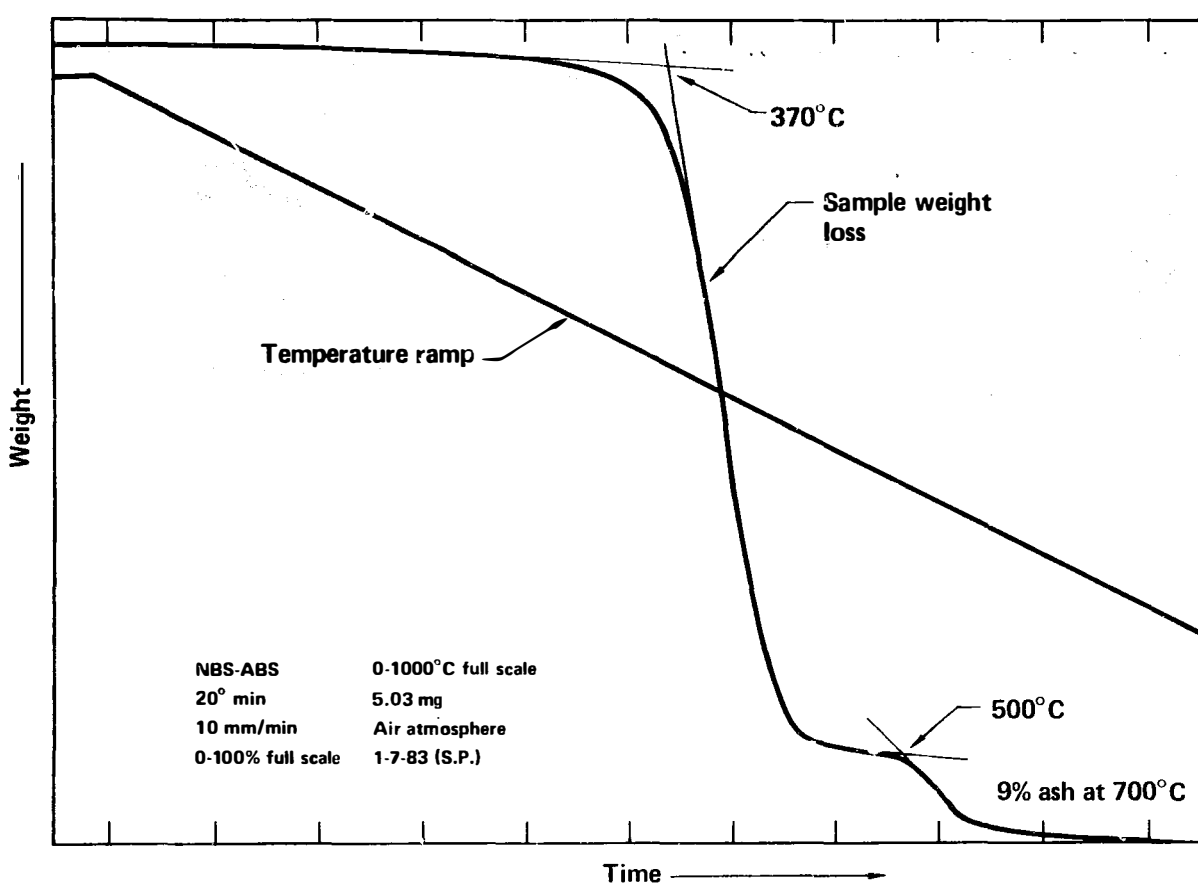


Figure 7. Thermogram of NBS-ABS.

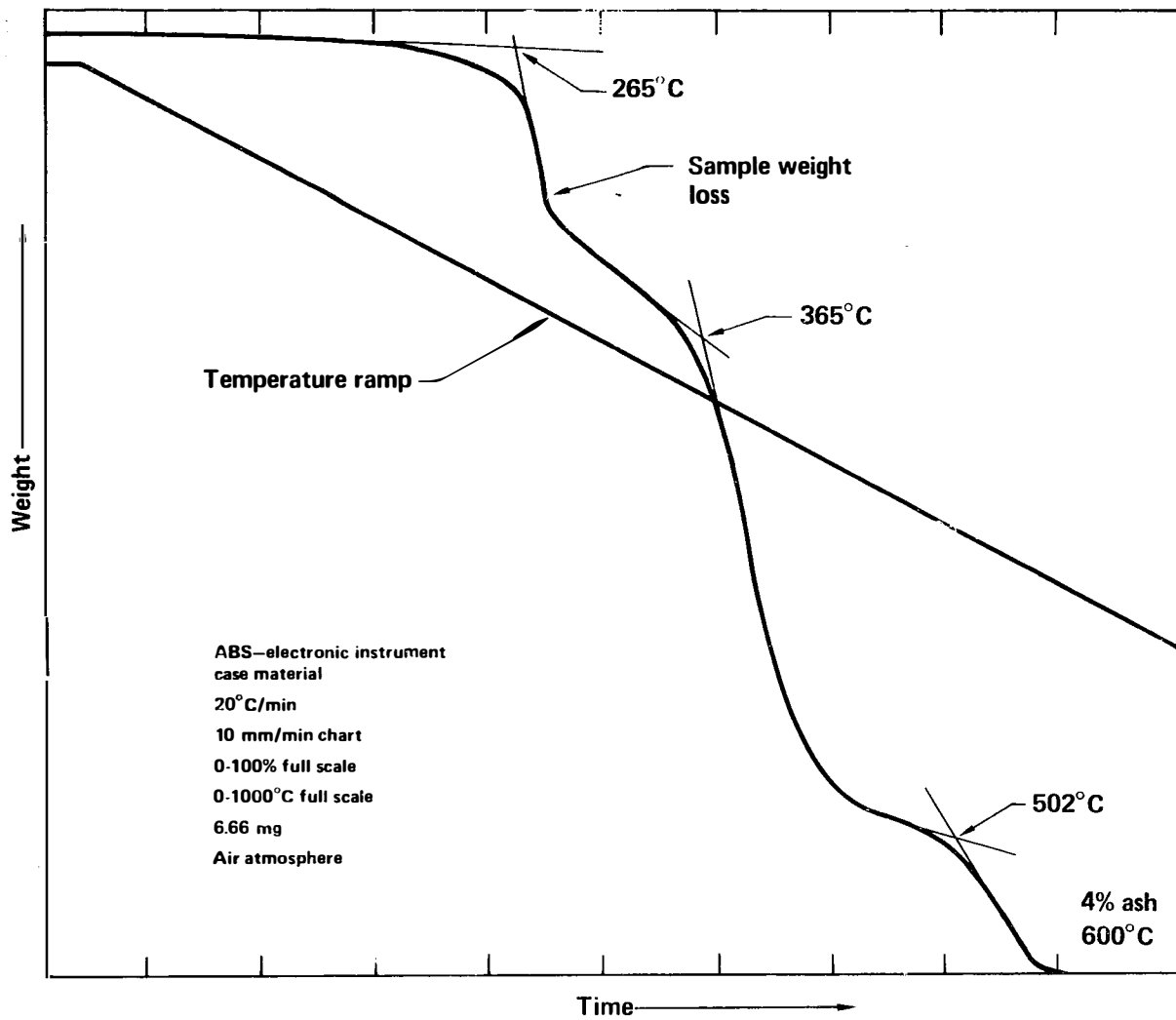


Figure 8. Thermogram of instrument-case ABS.

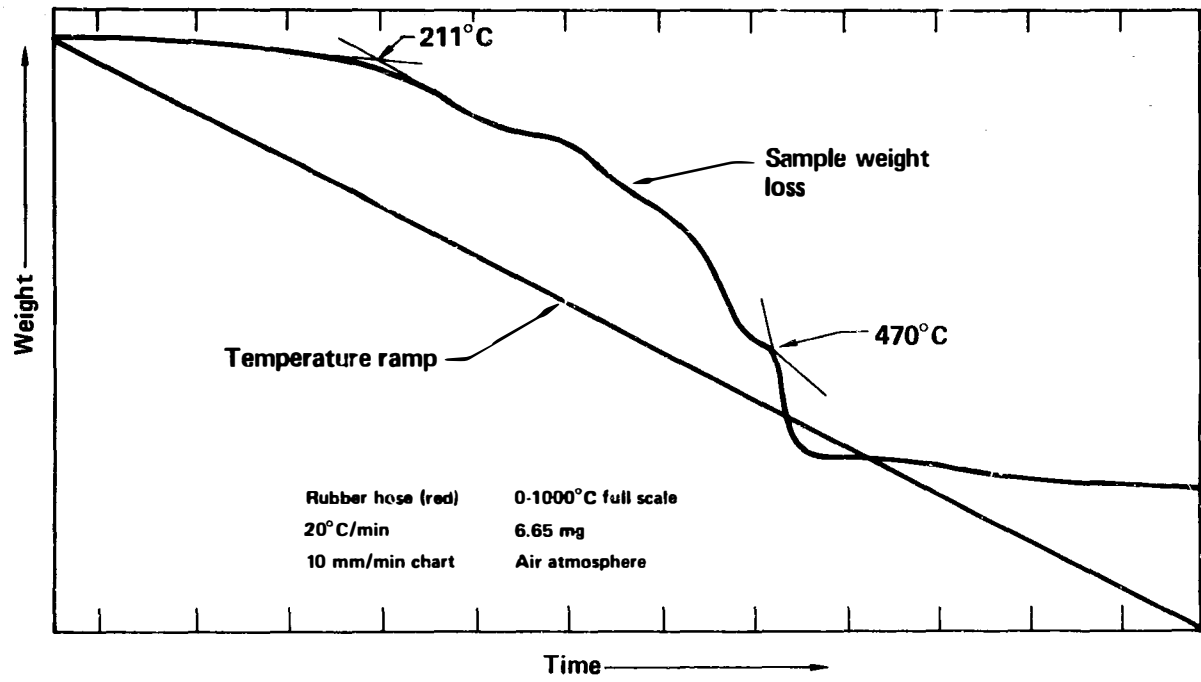


Figure 9. Thermogram of red rubber fire hose.

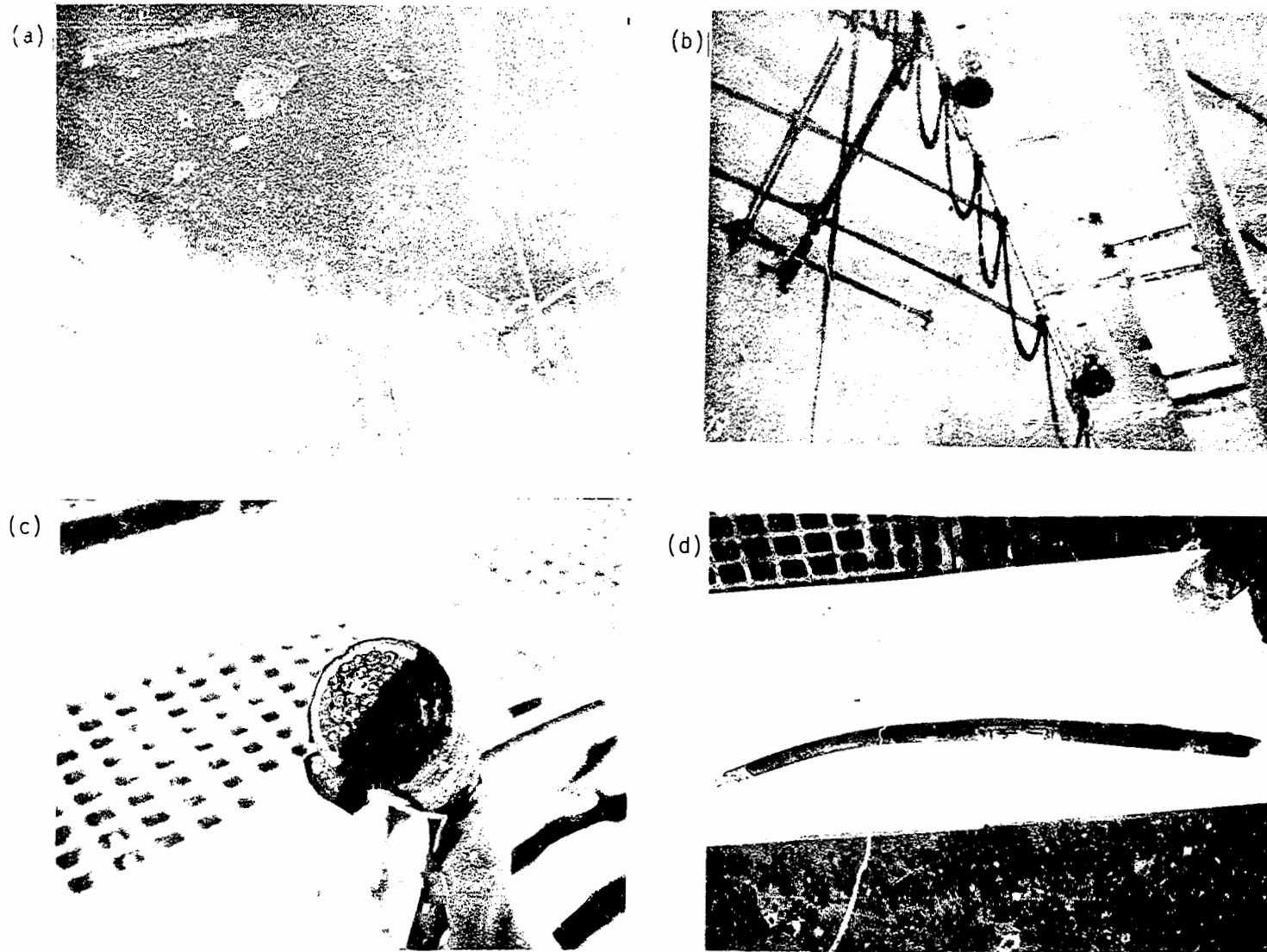


Figure 10. In-containment views and sectional pieces of the polar crane pendant: (a) Jib crane; D-ring A is in lower right. (b) Girder A of the polar crane. (c) North side of cable is ash; plastic tape is charred all around; no degradation under the tape. (d) Half of circumference is ash, half char (ash is gray, char black).

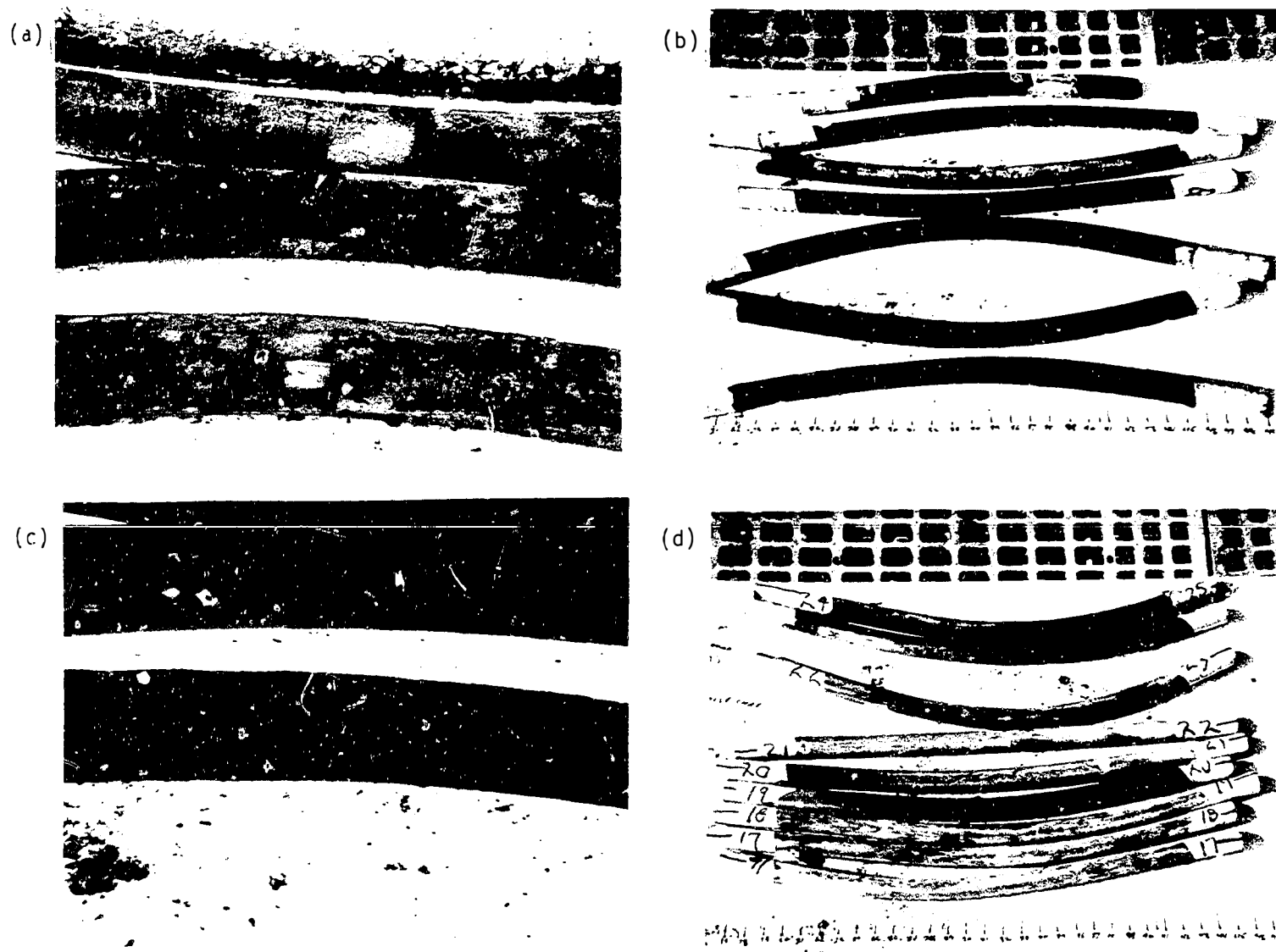
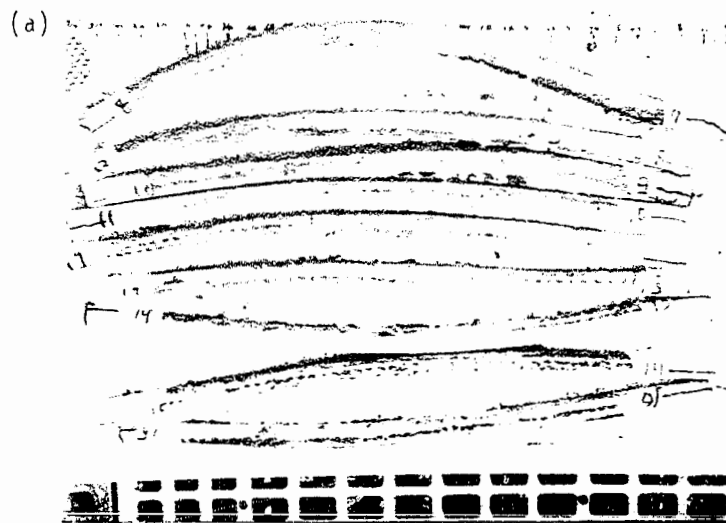


Figure 11. Sections from the top part of the polar crane pendant: (a) Low end is complete char; remainder is one side char, one side ash. (b) Cables 31-26; the higher the cable number, the higher it was on the polar crane pendant. (c) Char around complete circumference. (d) Cables 25-17.



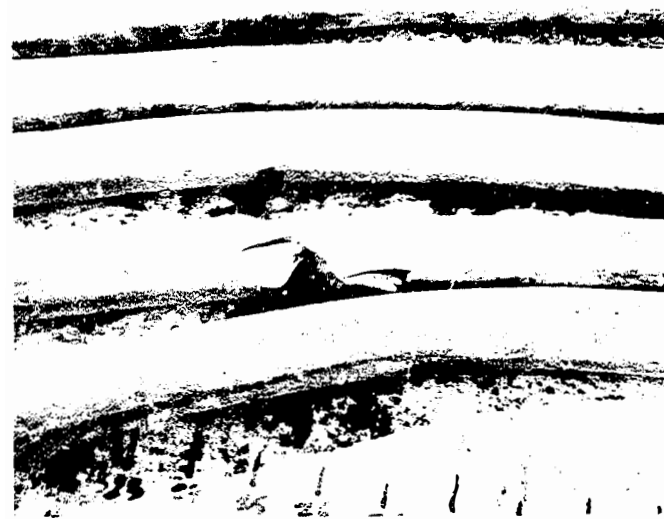
(a)



(b)



(c)



(d)

Figure 12. Sections from the bottom part of the polar crane pendant: (a) Cables 16-8. (b) Reverse sides of cables in (a). (c) Lengths 3-5, showing insulation cuts and checks. (d) Lengths 8-9, showing charred cut.

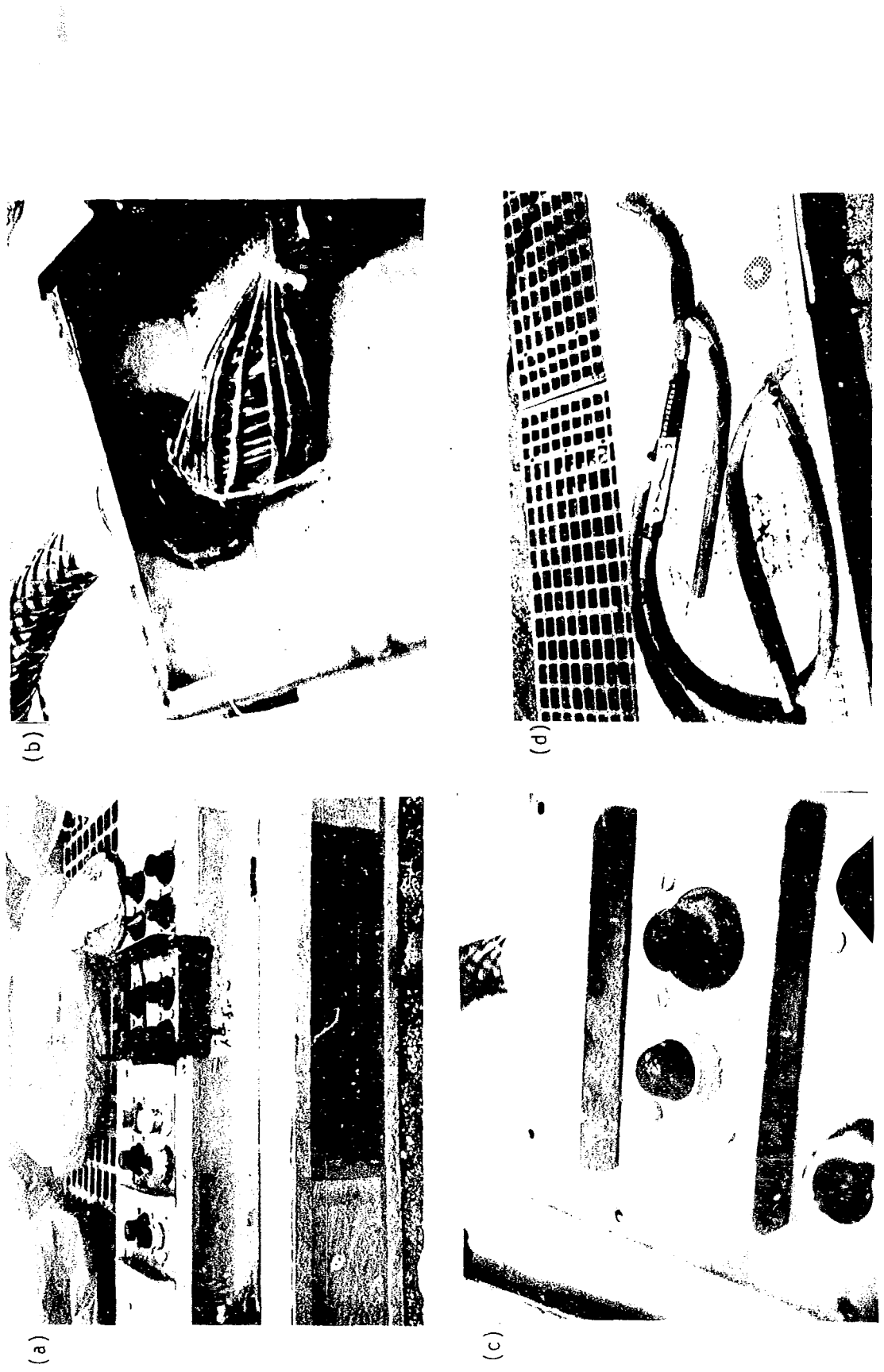


Figure 13. Details of control box and proximate cable.

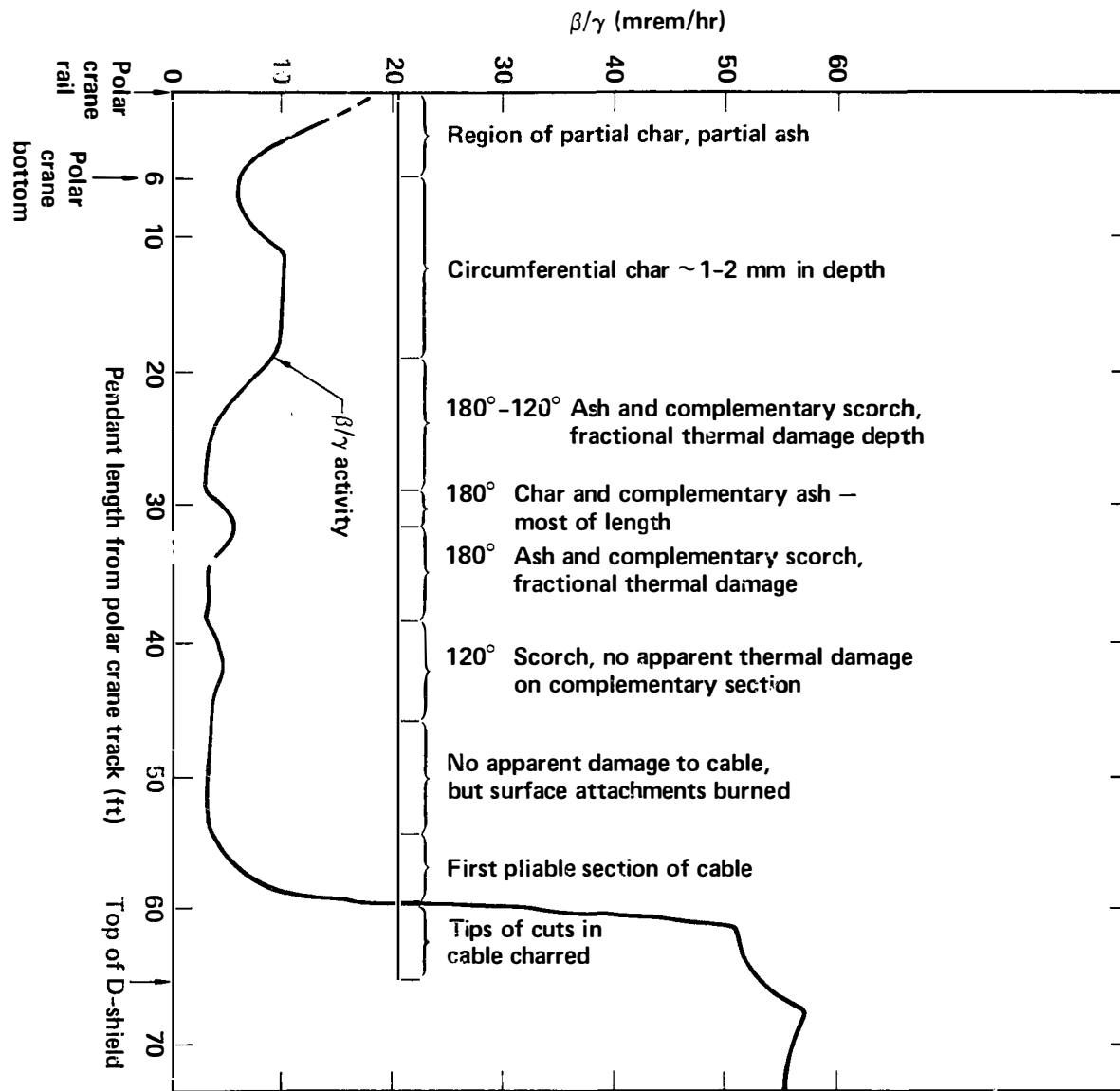


Figure 14. Distribution of residual radiation and burn damage along pendant length from the polar crane track.

46

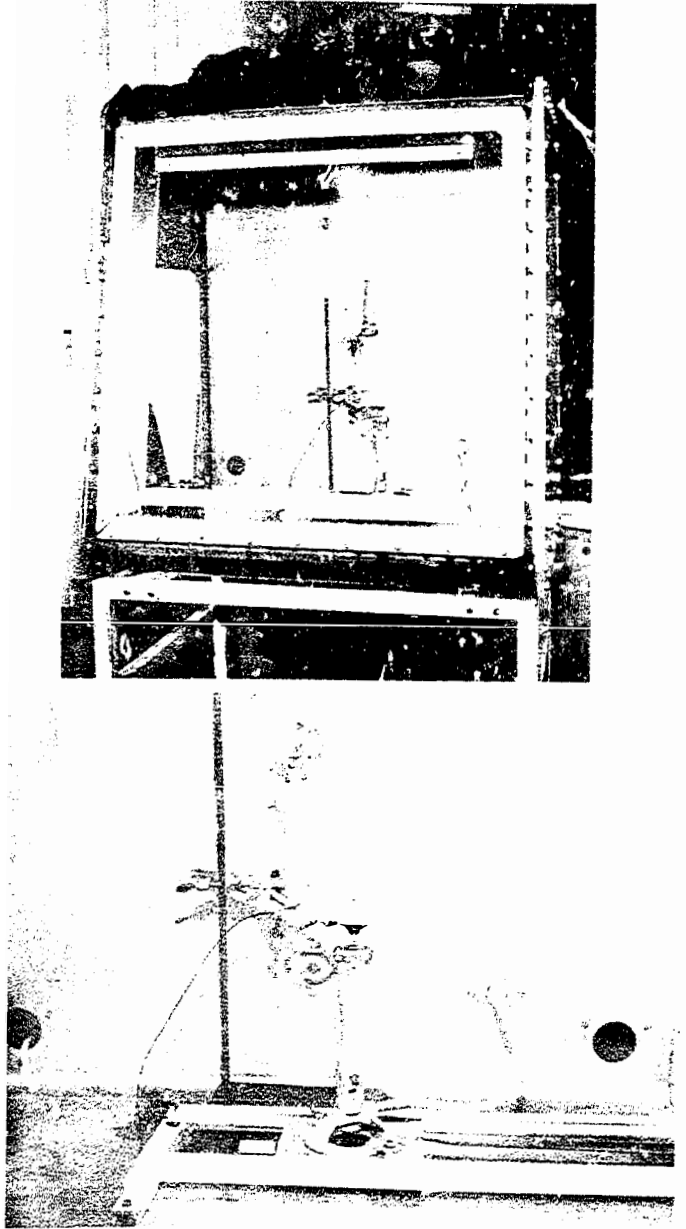


Figure 15. Small-scale materials and test apparatus for TMI exemplar materials. Hydrogen flame output was 6 W.



Figure 16. Comparison of exemplar polyethylene rope exposed to  $180 \text{ J/cm}^2$  for 30 s (left) and TMI-2 polyethylene rope (right).

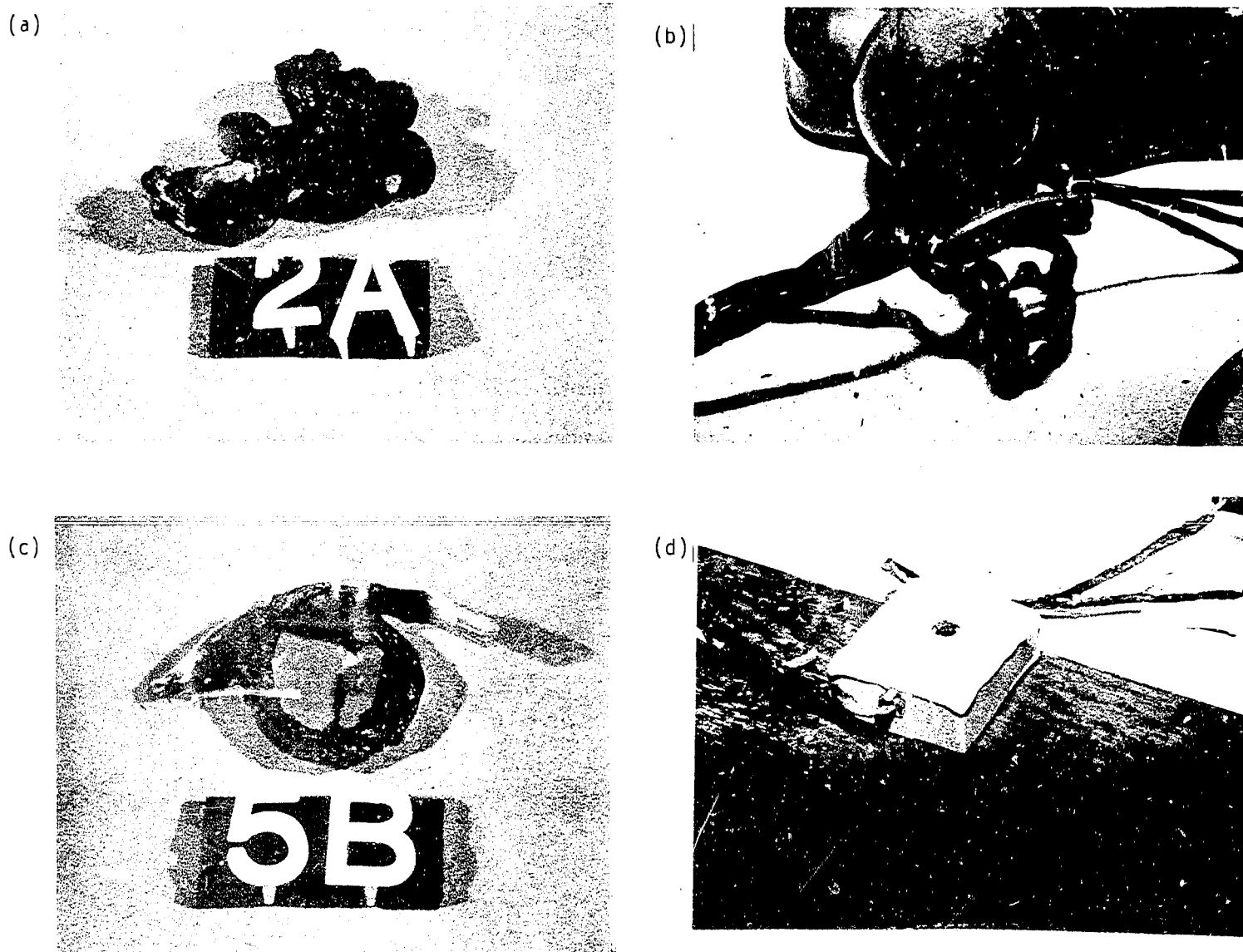


Figure 17. Comparison of exemplars exposed to  $180 \text{ J/cm}^2$  for 30 s and TMI materials: (a) Exemplar telephone receiver cord. (b) TMI receiver cord. (c) Exemplar extension cord. (d) TMI extension cord.

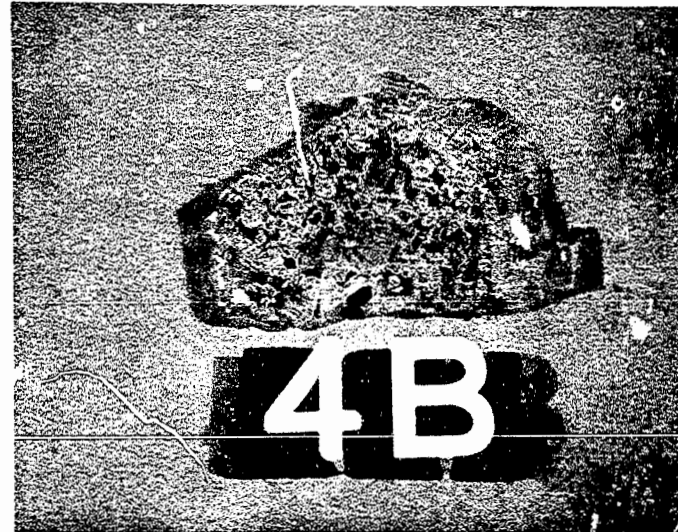


Figure 18. Comparison of exemplar acrylic exposed to  $180 \text{ J/cm}^2$  for 30 s (left) and TMI-2 telephone dial.

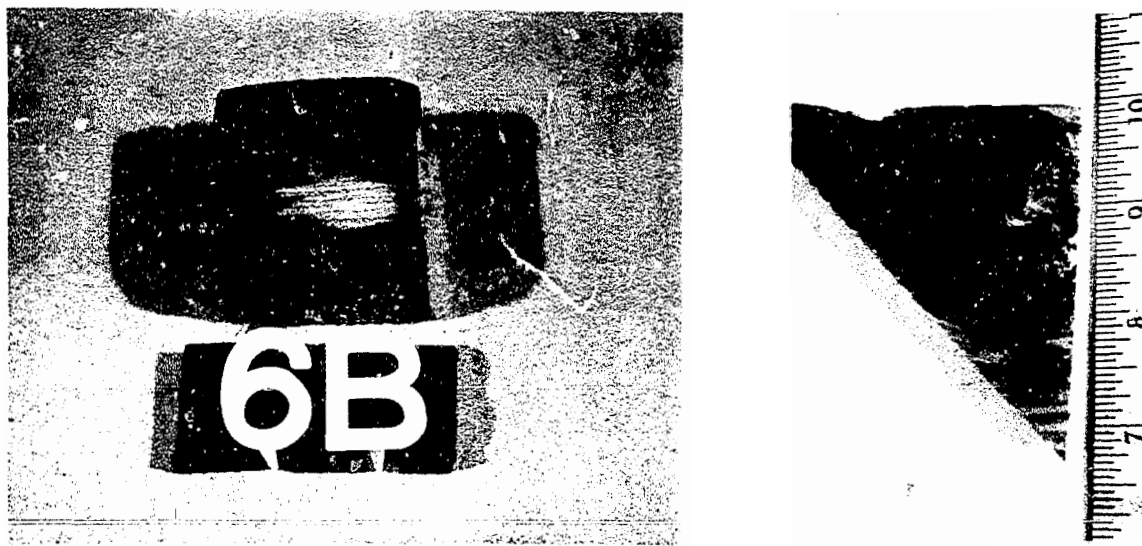


Figure 19. Comparison of exemplar plywood (fir) exposed to  $180 \text{ J/cm}^2$  for 30 s (left) and plywood from TMI.



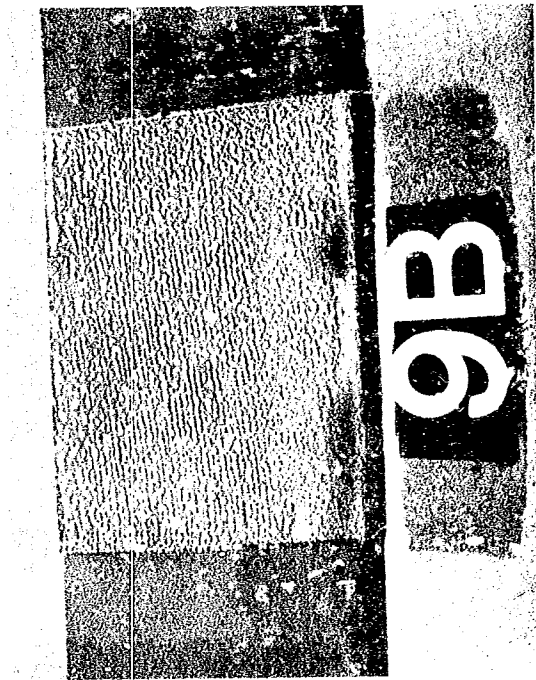
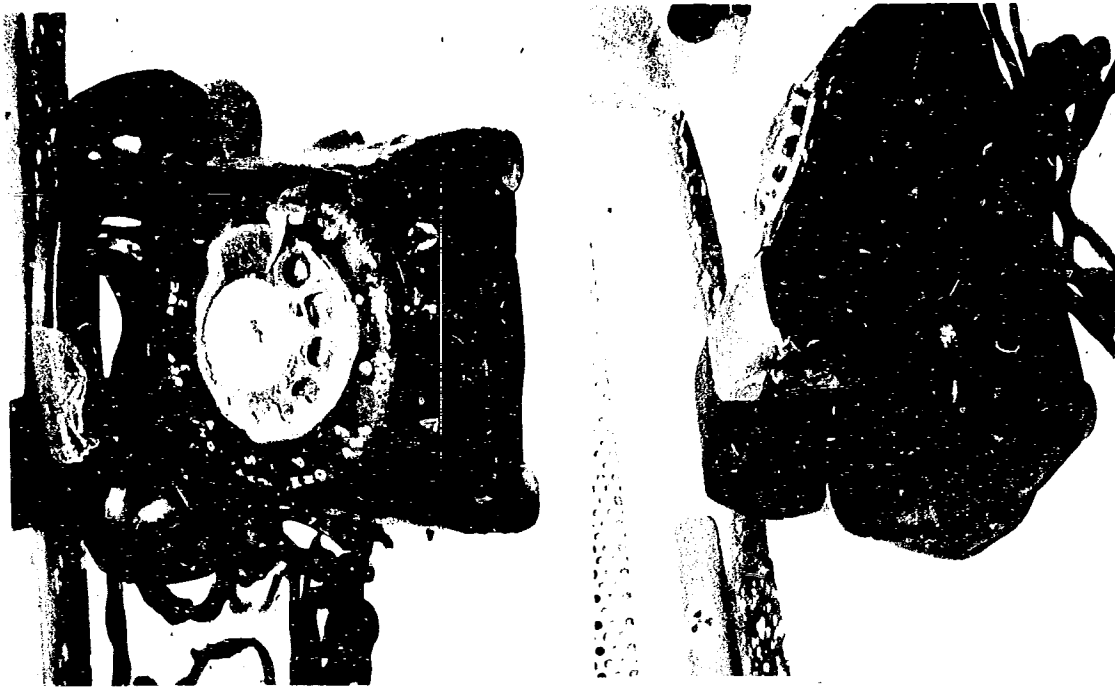


Figure 20. Comparison of exemplar duct tape exposed to  $120 \text{ J/cm}^2$  for 20 s (left) and TMI-2 duct tape.

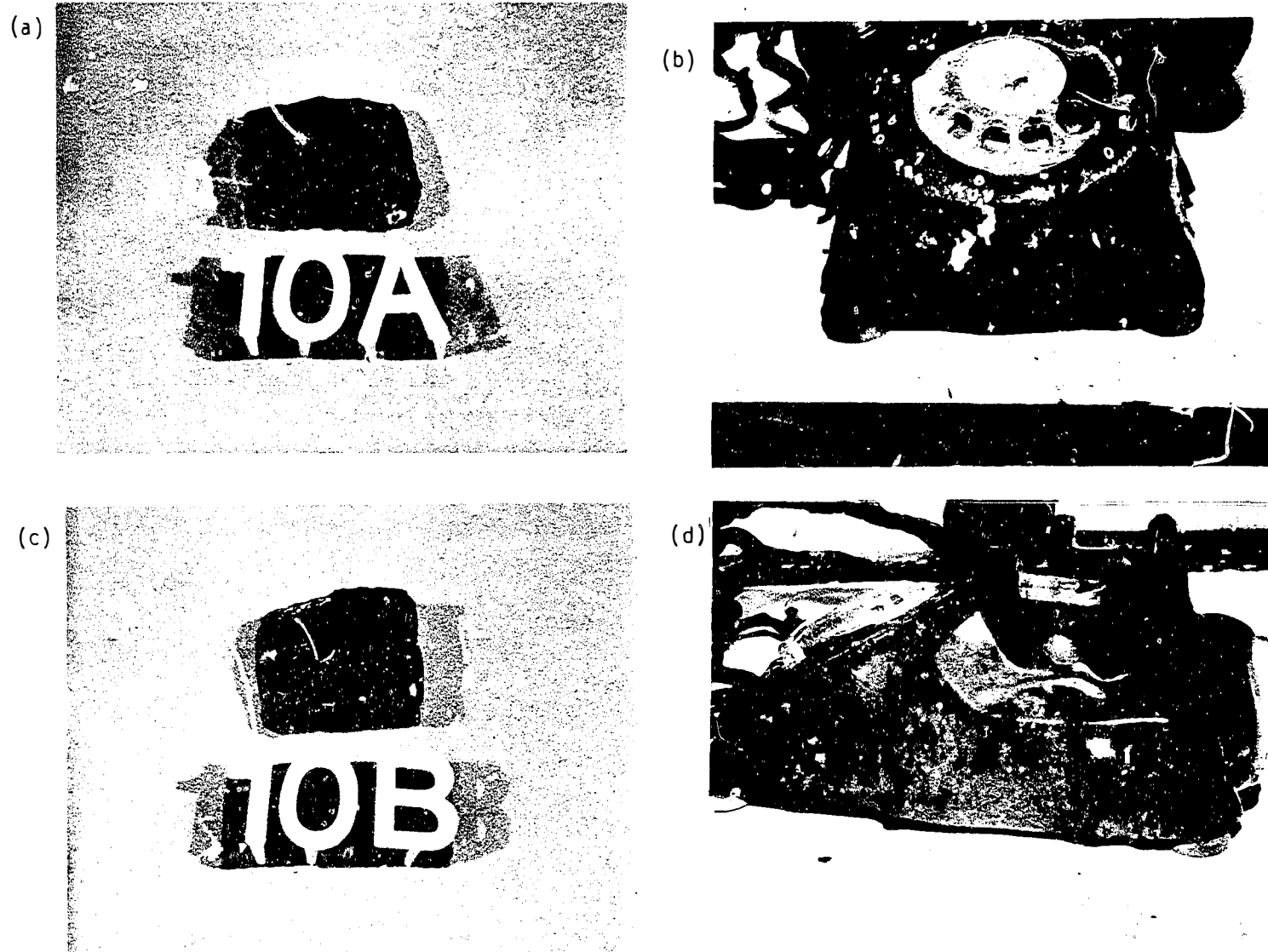
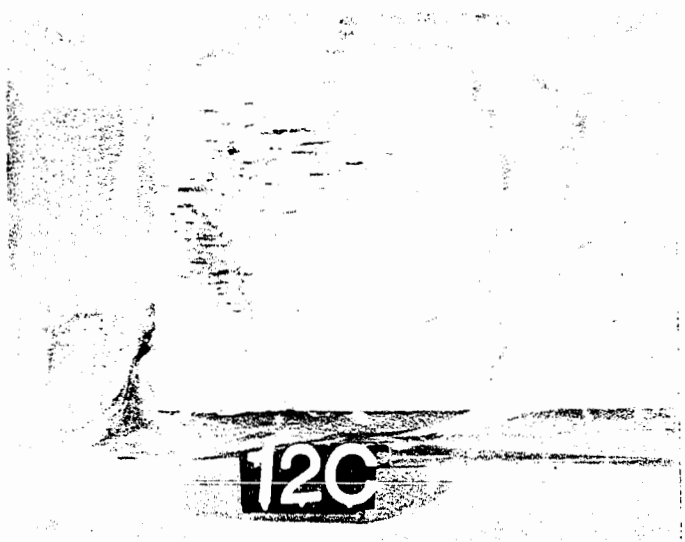


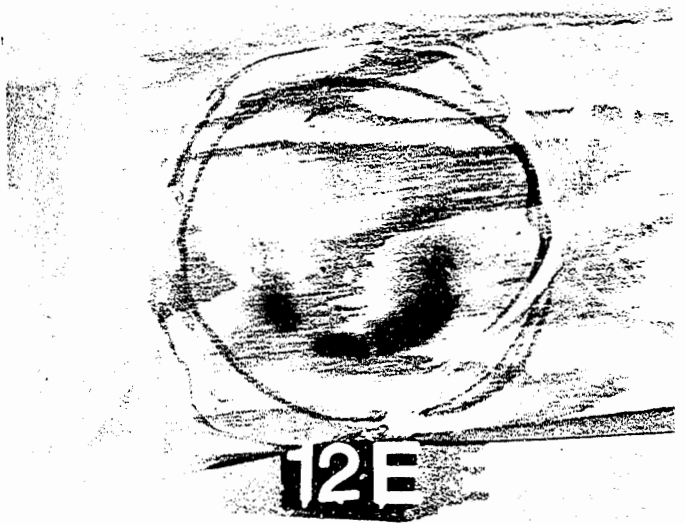
Figure 21. Comparison of exemplar telephone body pieces and TMI-2 ABS telephone body: (a) Exemplar exposed to  $120 \text{ J/cm}^2$  for 20 s. (b) Telephone from TMI. (c) Exemplar exposed to  $72 \text{ J/cm}^2$  for 12 s. (d) Telephone from TMI.

53

(a)



(b)



(c)

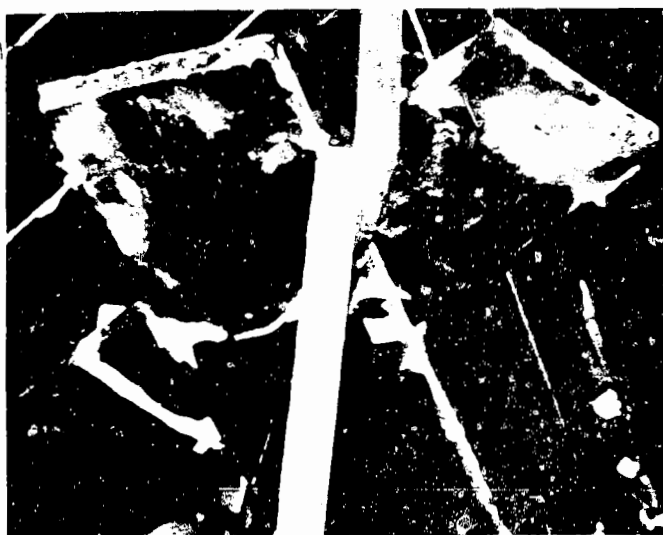


Figure 22. Comparison of exemplars and TMI-2 polyethylene-wrapped plywood: (a) Exemplar exposed to  $75 \text{ J/cm}^2$  for 12.5 s. (b) Exemplar exposed to  $78 \text{ J/cm}^2$  for 13 s. (c) Scaffolding at TMI.

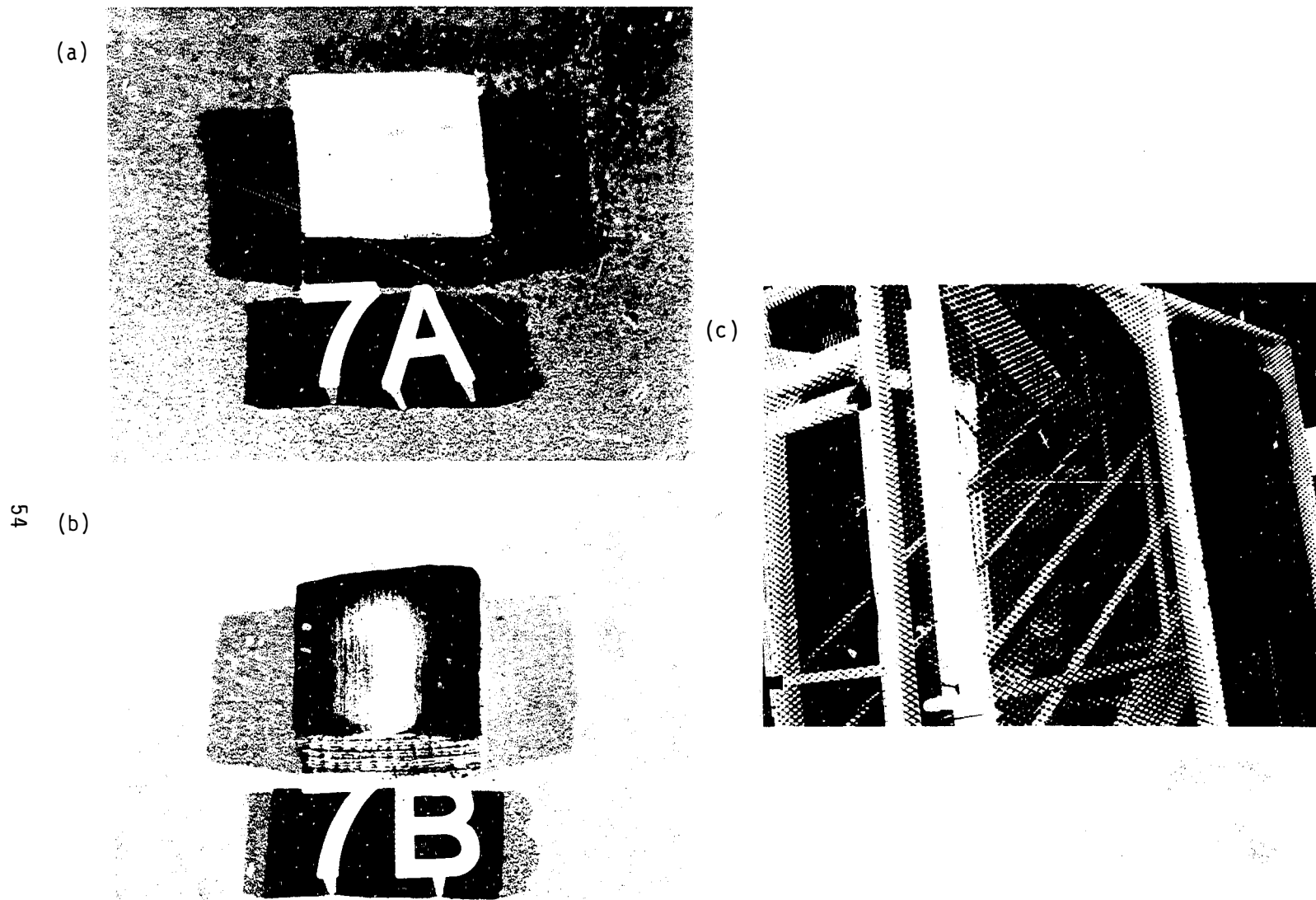


Figure 23. Comparison of exemplar wet plywood and TMI-2 wet plywood: (a) Exemplar exposed to 180  $\text{J}/\text{cm}^2$  for 30 s. (b) Exemplar exposed to 360  $\text{J}/\text{cm}^2$  for 1 min. (c) Plywood-framed cage at TMI.

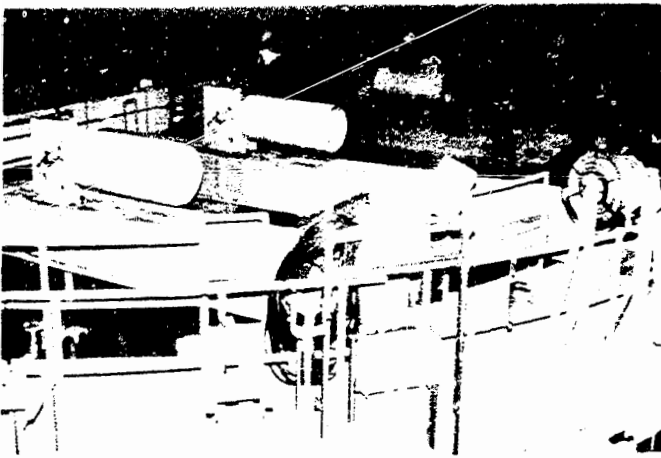
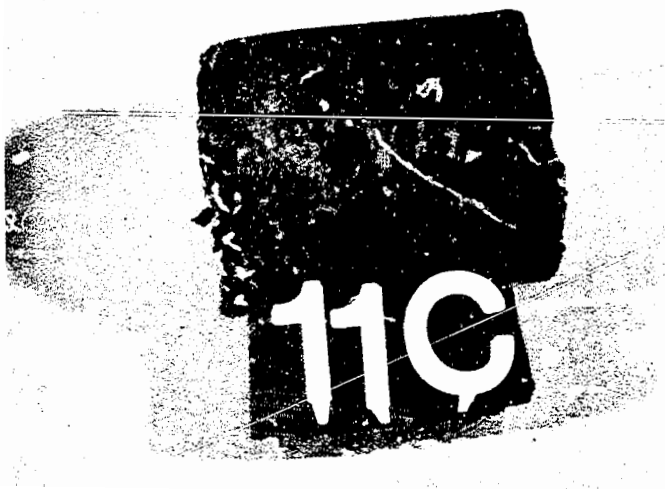


Figure 24. Exemplar red rubber fire hose exposed to  $360 \text{ J/cm}^2$  for 1 min (left) and fire hose at TMI (right).